

## Morphological development of the tidal inlet systems in the Wadden Sea



## Morphological development of the tidal inlet systems in the Wadden Sea

### Author(s)

Zheng Bing Wang

Ymkje Huisman

Ad van der Spek

## Morphological development of the tidal inlet systems in the Wadden Sea

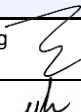



<b>Client</b>	Rijkswaterstaat Noord Nederland in cooperation with "Staf Deltacommissaris"
<b>Contact</b>	Robert Zijlstra (RWS-NN)
<b>Reference</b>	KPP ondersteuning staf Deltacommissaris, KPP Kustgenese 2
<b>Keywords</b>	Wadden Sea; Sea-level rise; morphological changes; ASMITA modelling

### Document control

<b>Version</b>	1.1
<b>Date</b>	03-07-2020
<b>Project nr.</b>	11203724-012
<b>Document ID</b>	11203724-012-BGS-0002
<b>Pages</b>	36
<b>Status</b>	final

### Author(s)

	Zheng Bing Wang	
	Ymkje Huismans	
	Ad van der Spek	

Doc. version	Author	Reviewer	Approver	Publish
0.1	Zheng Bing Wang 	Edwin Elias 	Toon Segeren 	
	Ymkje Huismans 			
	Ad van der Spek			

# Executive summary

Sea-level rise (SLR) in the Dutch Wadden Sea area is expected to accelerate. This will have an influence on morphological development of the Wadden Sea and as a consequence its ecological system. A feared effect of accelerated SLR is the disappearance of the ecologically valuable intertidal flats. To study the impact of accelerated SLR on the sediment dynamics of the Wadden Sea, simulations were carried out with the reduced complexity model ASMITA, within the framework of KUSTGENESE 2 ("Sediment exchange between the Wadden Sea and North Sea Coast, Modelling based on ASMITA", 1220339-008-ZKS-0006). Focus within that project was the impact on the sediment exchange through the inlets. In this study, these ASMITA results are further analysed, to infer the impact of SLR on the ebb-tidal delta, the channels and specifically the intertidal flats.

The ASMITA simulations are based on four future sea-level rise scenarios. One with a stable rate of 2 mm/year (current rate), and three scenarios with accelerated sea level rise rates, increasing from current rate of 2 mm/year to 4, 6 and 8 mm/year. Resulting sea level rise between 2020 and 2100 is respectively 16 cm, 29 cm, 40 cm and 49 cm. These scenarios cover the range between the RCP2.6 and RCP4.5 scenarios as presented by Vermeersen et al. (2018). Based on the analysis of the ASMITA results, it is concluded that the import rates to the Wadden Sea basins through the inlets show a delayed response to accelerated sea level rise. Because the import rates do not immediately increase, the amount of sediment available for sedimentation in the basins is not sufficient to keep up with sea level rise, which leads to losses of intertidal flats. As a consequence, the intertidal flat losses are very sensitive to the sea level rise scenario, while the import rates are not.

For the considered SLR scenarios and timeframe (2020 - 2100), complete drowning (i.e. loss of all intertidal flats) will occur in none of the tidal basins in the Dutch Wadden Sea. The area loss of the intertidal flats will be noticeable in 2100 for the highest SLR scenario (SLR80) and will be largest in the two larger basins in the western part, with predicted losses of intertidal area of about 15% in the Marsdiep and the Vlie inlets. In the smaller basins, Eierlandse Gat, Pinkegat and Zoutkamperlaag, the effects of SLR acceleration on the area loss of intertidal flats are less (<5%), according to the model results. However, the loss in averaged flat height is more noticeable in these smaller basins, up to almost 10% in 2100 for the SLR80 scenario.

The model ASMITA does not spatially differentiate within the basins. To get an idea on where the largest losses of intertidal area may occur, a system analysis of the Holocene tidal basin evolution was carried out. This suggests that the effect of accelerated SLR will be most noticeable in the area between the flood-tidal delta and the sea dikes or reclamation works along the main land coast.

# About Deltares

Deltares is an independent institute for applied research in the field of water and the subsurface. Throughout the world, we work on smart solutions, innovations and applications for people, environment and society. Our main focus is on deltas, coastal regions and river basins. Managing these densely populated and vulnerable areas is complex, which is why we work closely with governments, businesses, other research institutes and universities at home and abroad. Our motto is 'Enabling Delta Life'.

As an applied research institute, the success of Deltares can be measured by how much our expert knowledge can be used in and for society. At Deltares, we aim to use our leading expertise to provide excellent advice and we carefully consider the impact of our work on people and planet.

All contracts and projects contribute to the consolidation of our knowledge base. We always apply a long-term perspective when developing solutions. We believe in openness and transparency. Many of our software, models and data are freely available and shared in global communities.

Deltares is based in Delft and Utrecht, the Netherlands. We employ over 800 people from 40 countries. We have branch and project offices in Australia, Indonesia, New Zealand, the Philippines, Singapore, the United Arab Emirates and Vietnam. Deltares also has an affiliated organisation in the USA.

[www.deltares.nl](http://www.deltares.nl)

# Contents

	<b>Executive summary</b>	<b>4</b>
<b>1</b>	<b>Introduction</b>	<b>7</b>
1.1	Background / problem	7
1.2	Objectives	7
1.3	Approach and outline of the report	8
<b>2</b>	<b>Simulated morphological developments</b>	<b>9</b>
2.1	The used simulations	9
2.2	ASMITA model schematization	11
2.3	ASMITA results: development of intertidal flats	11
2.4	Development of tidal prism	12
2.5	Development of channels in the basins	13
2.6	Development of ebb-tidal deltas	14
<b>3</b>	<b>Interpretation of model results for tidal flat development</b>	<b>16</b>
3.1	Introduction	16
3.2	Interpretation based on ASMITA simulations	16
3.2.1	Method for translating volume changes to changes in area and average height	16
3.2.2	Development of intertidal area and flat height	19
3.3	Spatial distribution of tidal flats within the basins	25
3.3.1	Introduction	25
3.3.2	Pattern of sediment supply and distribution	26
3.3.3	Grain-size selection	27
3.3.4	Basin morphology under increasing sediment demand	28
3.4	Summary	28
<b>4</b>	<b>Discussions</b>	<b>30</b>
4.1	The analyzed ASMITA simulations	30
4.2	Model results	30
4.3	Uncertainties	32
<b>5</b>	<b>Conclusions and recommendations</b>	<b>34</b>
5.1	Conclusions for management	34
5.2	Recommendations	34
<b>6</b>	<b>References</b>	<b>36</b>

# 1 Introduction

## 1.1 Background / problem

Sea-level rise (SLR) in the Dutch Wadden Sea area is expected to accelerate, although the exact future development of the sea-level is uncertain (Vermeersen et al., 2018). An acceleration in SLR rate will have an influence on morphological development of the Wadden Sea and changes in morphology will impact its ecological functioning (Wang et al., 2018). A feared effect of accelerated SLR is the disappearance of the ecologically valuable intertidal flats. If the SLR rate exceeds the sedimentation rate in the basin, the amount of intertidal flat will decrease and the Wadden Sea will become deeper. A deeper Wadden Sea will increase the sediment import and the sedimentation rate will increase as well. If SLR stays below a critical level, a new dynamic morphological equilibrium can be established. However, if SLR rate exceeds the critical level, on the long term the Wadden Sea will drown and practically all intertidal flats disappear (Stive and Wang, 2003; Van Goor et al., 2003; Lodder et al., 2019). The critical SLR rates for the various tidal inlet systems in the Dutch Wadden Sea have been evaluated in the studies of Van Goor et al. (2003) and Wang et al. (2018). These studies show that the critical values are dissimilar for different inlet systems. In general, the critical values are higher for inlets with smaller back-barrier basins. The theoretical analysis by Lodder et al. (2019) provides initial insights on the transient development of a tidal basin when SLR rate changes. However, their analysis was based on a single element model. Therefore, the transient developments of the various morphological elements (ebb-tidal delta, channels and intertidal flats) in the various tidal inlet systems for future SLR scenarios are still not sufficiently studied.

Within the framework of the Kustgenese 2 project, ASMITA simulations for four SLR scenarios have been carried out to evaluate the future development of the sediment exchanges between the North Sea and the Dutch Wadden Sea. One with a stable rate of 2 mm/year (current rate), and three scenario's with accelerated sea level rise rates, increasing from current rate of 2 mm/year to 4, 6 and 8 mm/year. Resulting sea level rise between 2020 and 2100 is respectively 16 cm, 29 cm, 40 cm and 49 cm. The simulations are described in the report for Kustgenese 2 (Wang and Lodder, 2019). This study focused on the sediment exchange through the tidal inlets, i.e. import / export of sediment. In the models, the intertidal part (tidal flats) and the subtidal part (channels) are schematised into two separate elements. This means that the model results also contain information on the development of the intertidal flats in the Wadden Sea. This information is useful to evaluate the impact of accelerated SLR on the ecological functioning of the Wadden Sea. In this report, we therefore present a more detailed analysis of the evolution of the morphological elements.

## 1.2 Objectives

The aim of the present study is to obtain insights into the developments of the tidal inlet systems in the Dutch Wadden Sea, with special focus on the changes of the intertidal flats in the Wadden Sea, under influence of future SLR.

The study will focus on the following research questions:

- What are the expected changes of the intertidal flats, in terms of their volumes, areas and heights, for the various SLR scenarios?
- How will the channels in the Wadden Sea and the ebb-tidal deltas develop for the various SLR scenarios?

### 1.3 Approach and outline of the report

The present study is based on the analysis of the ASMITA model results, from the existing simulations carried out within the framework of the Kustgenese 2 project.

The ASMITA model output contains the time evolution of the volumes of the three morphological elements for each tidal inlet system, viz. the ebb-tidal delta, the channels and the intertidal flats in the back-barrier basin. Chapter 2 analyses first the direct output of the ASMITA simulations, i.e. the developments of the volumes of all morphological elements (intertidal flats, channels and ebb-tidal delta) in a tidal inlet system, as schematised in the ASMITA models. In Chapter 3 the development of the intertidal flats in the tidal basins are further evaluated by calculating their changes of the horizontal area and of the averaged height measured from the moving low water accounting SLR and changing tidal range. However, these results are basin-averaged values and do not show changes in the distribution of tidal flats over the back-barrier basin. Therefore, the understanding of tidal basin evolution under high rates of sea-level rise in the past is used to sketch the situation to be expected in case the sedimentation cannot keep pace with SLR. In Chapter 4 conclusions from the study are summarised and recommendations are given.



## 2 Simulated morphological developments

### 2.1 The used simulations

Four scenarios of SLR will be considered in the present study, with SLR rate in 2100 equal to 2, 4, 6 and 8 mm/y respectively. For the exact method on how the accelerated sea-level rise scenarios are constructed, reference is made to Vermeersen et al. (2018). Vermeersen presented three scenarios, see Figure 2.1. According to these scenario's the SLR rates in 2100 are respectively about 5, 7 and 12 mm/y. Further analysis on the variation of the SLR scenarios learned that in the three scenarios the SLR rate increases linearly in time until a maximum is reached (end of acceleration period). The rate of increase is higher, and the period of acceleration is longer for a higher scenario. The acceleration ends in 2030, 2060 and 2100 respectively for the three scenarios.

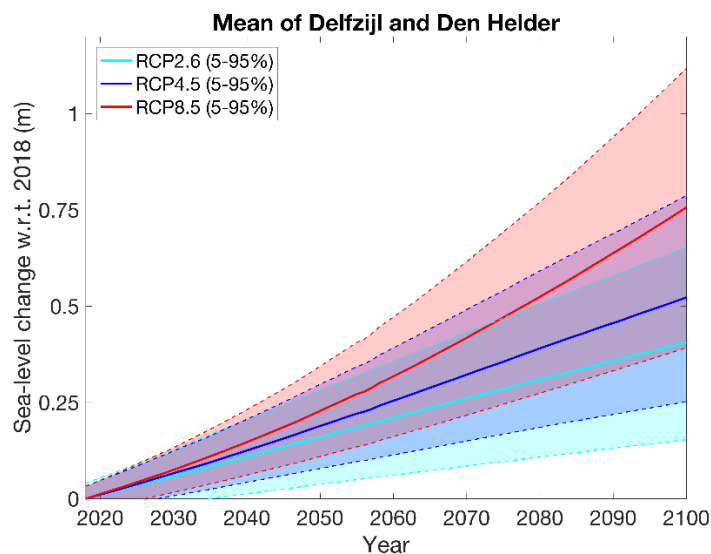


Figure 2.1 Sea-level rise scenarios presented in Vermeersen et al. (2018).

It is further noted that in the scenarios of Vermeersen et al. (2018), the acceleration of SLR started earlier than 2020, which is different from the scenarios defined here. Based on these considerations the four scenarios in the present study are exactly defined as follows (see Figure 2.2).

1. Continuation of the present SLR rate:  $R$  is constant and equal to 2 mm/y;
2.  $R=2$  mm/y until 2020, from 2020 to 2050  $R$  increases linearly to 4 mm/y, and then remain constant,  $R=4$  mm/y;
3.  $R=2$  mm/y until 2020, from 2020 to 2060  $R$  increases linearly to 6 mm/y, and then remain constant,  $R=6$  mm/y;
4.  $R=2$  mm/y until 2020, from 2020 to 2070  $R$  increases linearly to 8 mm/y, and then remain constant,  $R=8$  mm/y.

Scenario 1 is about the same as the RCP2.6 scenario in Vermeersen et al. (2018) and scenario 4 is comparable with the RCP4.5 scenario (see Fig.2.1).

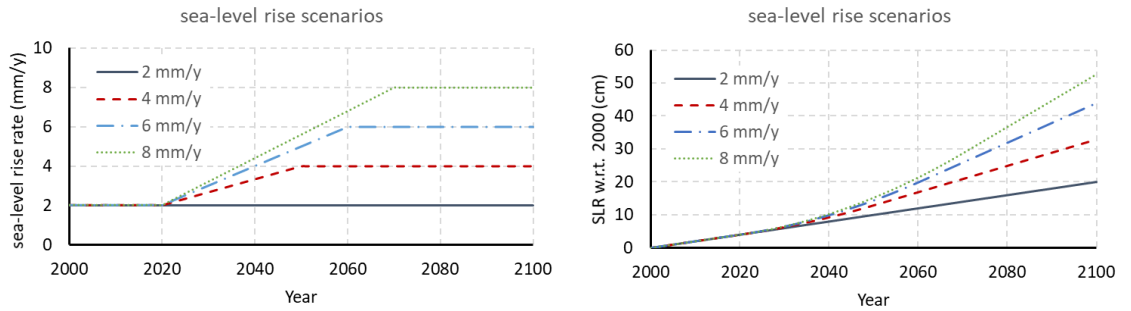


Figure 2.2 The four sea-level rise scenarios considered in the present study. Left: change of SLR rate; right: SLR since 2000.

Table 2.1 Input parameters of the ASMITA application models for the tidal inlets (symbols explained in chapter 2)

Inlet	Texel	Eierland	Vlie	Ameland	Pinkegat	Zoutkamp
Basic configuration: tidal range and the horizontal areas of the three elements						
$2a$ (m)	1.65	$F(t)^*$	1.90	2.15	2.15	2.25
$A_f$ (km <sup>2</sup> )	133	105	328	178	38.1	65
$A_c$ (km <sup>2</sup> )	522	52.7	387	98.3	11.5	40
$A_d$ (km <sup>2</sup> )	92.53	37.8	106	74.7	34	78
Parameters influencing morphological timescale						
$n$ (-)	2	2	2	2	2	2
$C_E$ (-)	0.0002	0.0002	0.0002	0.0002	0.0002	0.0002
$w_{sf}$ (m/s)	0.0001	0.0001	0.0001	0.0001	0.0001	0.0001
$w_{sc}$ (m/s)	0.0001	0.00005	0.0001	0.00005	0.0001	0.0001
$w_{sd}$ (m/s)	0.00001	0.00001	0.00001	0.00001	0.00001	0.00001
$\delta_{od}$ (m <sup>3</sup> /s)	1550	1500	1770	1500	1060	1060
$\delta_{dc}$ (m <sup>3</sup> /s)	2450	1500	2560	1500	1290	1290
$\delta_{cf}$ (m <sup>3</sup> /s)	980	1000	1300	1000	840	840
Initial conditions: volumes of the three morphological elements in 1970						
$V_{f0}$ (Mm <sup>3</sup> )	51.5	55	162	120	29.6	69
$V_{c0}$ (Mm <sup>3</sup> )	2160	106	1230	302	18.5	177
$V_{d0}$ (Mm <sup>3</sup> )	509.1	132	369.7	131	35	151
Parameters for defining the morphological equilibrium						
$V_{fe}$ (Mm <sup>3</sup> )	87.78	57.83	250	131.2	30.3	70
$\alpha_c$ (10 <sup>-6</sup> )	15	13.13	9.6	10.241	10.14	27.266
$\alpha_d$ (10 <sup>-3</sup> )	4.025	8	2.662	2.92157	6.9278	9.137

\* For the Eierlandse Gat inlet the tidal range is set as function of time: it increases linearly from 1.73 m in 1970 with 3 mm per year.

In the study of Wang and Lodder (2019) the four SLR scenarios were first simulated with the ASMITA models with the existing parameter setting (see Wang et al., 2006) before the parameter setting for the three inlets in the Western part of the Dutch Wadden Sea were adjusted to obtain better agreement between the model results and the insights from the recent analysis of bathymetric data (Elias, 2019). Here we only analyse the model results after the parameter setting adjustment. All the input parameters are given in Table 2.1.

## 2.2 ASMITA model schematization

In the ASMITA models used, a tidal inlet system is schematised in three morphological elements: (1) the intertidal flats, (2) the channels in the back-barrier basin, and (3) the ebb-tidal delta. The used state variable for these morphological elements are defined as follows:

- Volume of the intertidal flats  $V_f$ : this is the volume of sediment between the moving Low Water (LW) and High Water (HW). Note that sea-level rise is considered as an upwards shifting of the tidal frame, thus LW and HW. Sea-level rise thus results in a decrease of  $V_f$ , calculated as the horizontal area of the intertidal flats  $A_f$  multiplied by the sea-level rise.
- Volume of the channels  $V_c$ : this is the water volume below LW in the back-barrier basin. Sea-level rise causes an increase of  $V_c$  equal to the horizontal area of the channels  $A_c$  multiplied by the sea-level rise.
- Volume of the ebb-tidal delta  $V_d$ : this is the sediment volume above the normal coastal profile. Sea-level rise causes a decrease of  $V_d$  equal to the horizontal area of the ebb-tidal delta  $A_d$  multiplied by the sea-level rise.

The values of these state variables are calculated at each time step of the simulations and recorded as function of time in the model output. The simulated changes of these variables are the results of the direct effect of sea-level rise as explained above and the effect of sedimentation / erosion. In the following sections the model results, according to the direct model output, are presented first. Furthermore, the tidal prism  $P$ , as used in the model for evaluating the morphological equilibrium, is also presented. It is assumed that the tidal basins are much shorter than the tidal wave, so that  $P$  and  $V_f$  are related to each other:

$$P = 2aA_b - V_f = 2a(A_f + A_c) - V_f \quad (2-1)$$

Herein  $a$  is the tidal amplitude and  $A_b$  is the horizontal area of the back-barrier basin.

## 2.3 ASMITA results: development of intertidal flats

The simulated volume development of the intertidal flats of the six tidal inlet systems are depicted in Fig.2.3. Note that the simulations started in 1970, the figure presents results after 2000 and the differences between the SLR scenarios start in 2020. The following observations are made:

- For most of the tidal inlets limited changes of the intertidal flats volume is predicted by the model if the present SLR rate will continue (SLR20). Only in the basin of the Texel Inlet the change will be well noticeable. The volume of the intertidal flats will increase in the future according to the model results, which is a response to the disturbance caused by the closure of the Zuiderzee.
- For all the tidal inlet systems there is a clear difference in the development of the intertidal flats between the four SLR scenarios. The differences follow the SLR scenarios (compare with Fig.2.2). Note that this is consistent with the conclusion drawn on the development of the differences in the sediment exchange through the inlets (Wang and Lodder, 2019): delay in sediment transport between the morphological elements and thus in the sedimentation-erosion means that the direct effects of SLR on the volumes of the morphological elements are dominant in the first period after the acceleration of SLR.
- Accelerated SLR will cause losses of intertidal flats. The volume changes of the flats, for a same SLR scenario, are different for the different tidal inlets, in absolute sense ( $m^3$ ) as well as relative sense (%). For the highest SLR scenario (SLR80) the relative losses from 2020 to 2100 are about 10%, 7%, 20%, 25%, 15%, and 20% for the inlets Zoutkamperlaag, Pinkegat, Ameland, Vlie, Eierlandse Gat and Texel respectively. The general trend is that for the larger back-barrier basins, the effect of accelerated sea-level rise on the intertidal flats is larger. This agrees with the conclusion from the theoretical analysis (Wang and Lodder, 2019; Lodder et al., 2019): For the larger basins the critical SLR rate is lower, and it is the magnitude of the dimensionless SLR rate (the ratio between the SLR rate and the critical rate) that determines the effects of SLR.
- The general trend mentioned in the previous points does not explain all the model results. As an example, the relative loss in the Texel Inlet is about the same as in the Ameland Inlet

although the critical SLR rate for the Texel Inlet is much lower (Wang et al., 2018). This deviation from the general trend is due to the difference in the initial state between the two inlet systems. Due to the closure of the Zuiderzee, the amount of the intertidal flats in Texel Inlet is already much lower than at morphological equilibrium. This explains also why the intertidal flats volume stabilizes in relative short time, i.e. dynamic equilibrium for SLR40. In this scenario the SLR rate will increase to 4 mm/year, which is still below the critical level. As pointed out by Wang and Lodder (2019), the time process for achieving the dynamic equilibrium (cq. drowning when the critical SLR rate is exceeded) depends on the corresponding morphological time scale (with respect to dynamic equilibrium) as well as the initial morphological state (see also Lodder et al., 2019).

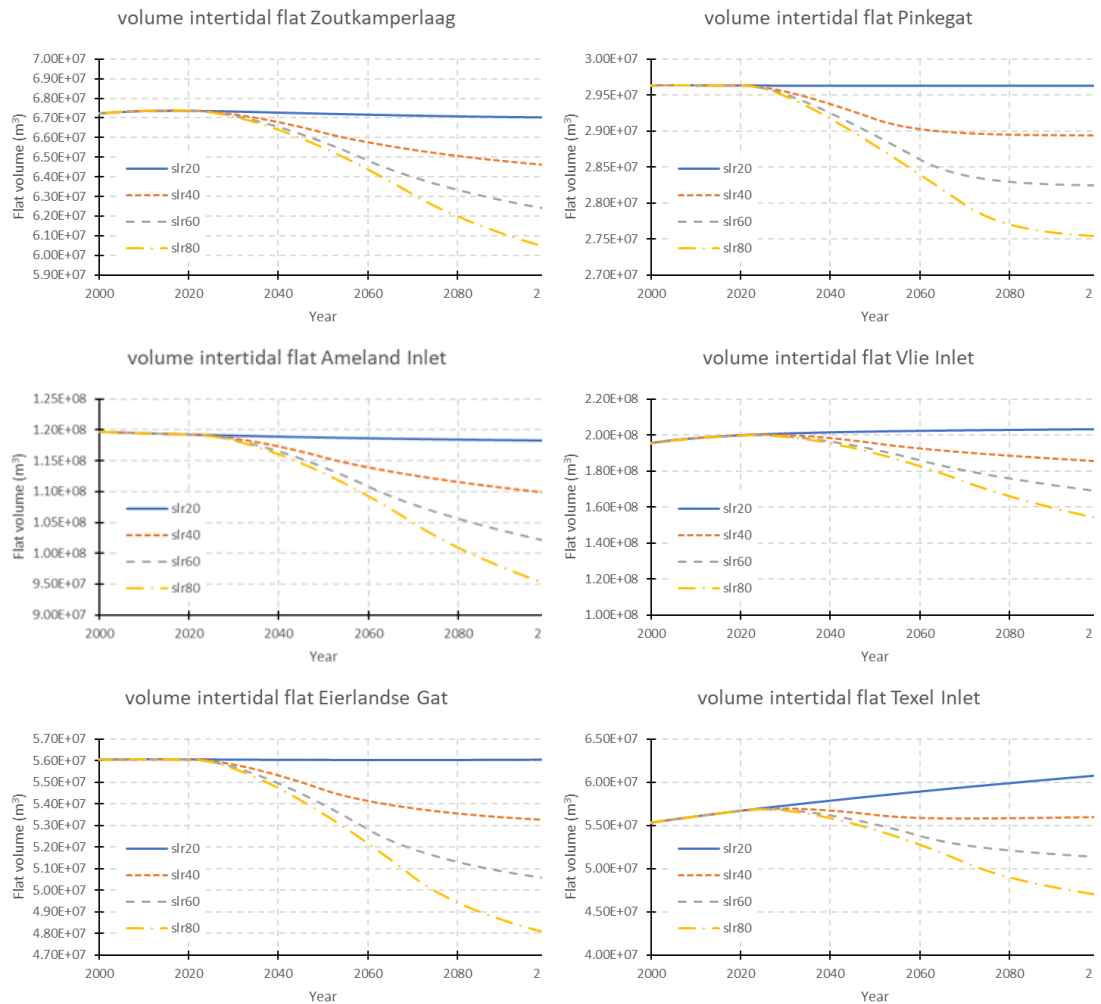


Figure 2.3 Simulated developments of the volumes of the intertidal flats in the back-barrier basins.

## 2.4 Development of tidal prism

The development of the tidal prisms of the six tidal inlet systems is presented in Figure 2.4. We present these results before the development of the other two morphological elements in each tidal inlet system for two reasons. Firstly, the development of the tidal prism is directly related to that of the intertidal flats (see Eq. 2-1) as the pumping mode (water level in the basin is constant in space and only varies with time), applicable for short basins, is assumed. Secondly, the development of the tidal prism influences the developments of the channels and the ebb-tidal delta via the empirical relation determining their equilibrium volumes.

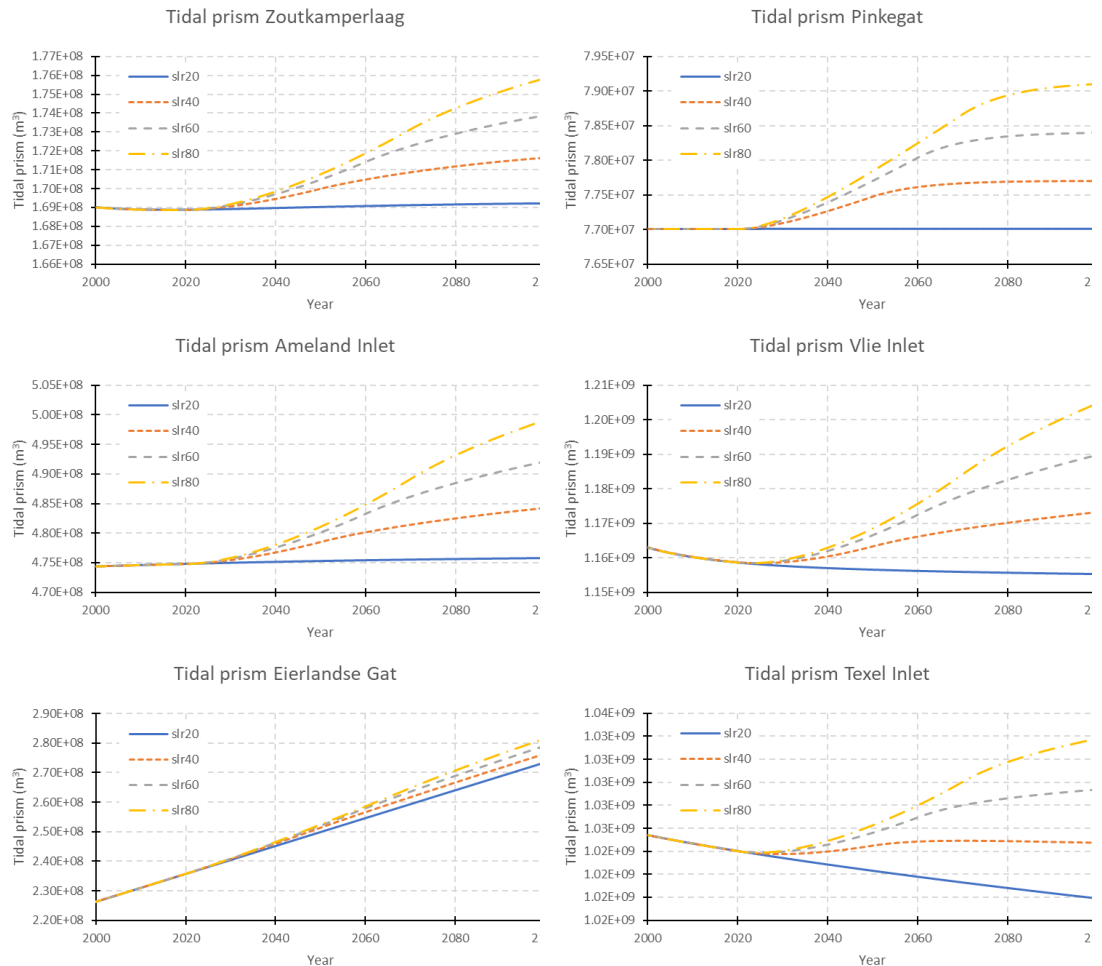


Figure 2.4 Simulated developments of the tidal prisms of the tidal inlet systems.

For five of the six inlets the development of the tidal prism shows a mirrored image of the development of the intertidal flats. As the tidal range is kept constant during the whole simulation period, every  $\text{m}^3$  decrease in flat volume means a  $\text{m}^3$  increase of the tidal prism. The only exception is the Eierlandse Gat Inlet, in which the tidal range is set to increase linearly in time (see Wang and Lodder, 2019). The development of the tidal prism in this inlet is a combined effect of the increase of the tidal range and the decrease of the tidal flat volume (Eq. 2-1). Note that the increase of the tidal range in the model is for representing the increase of the basin area in reality.

## 2.5 Development of channels in the basins

The development of the volumes of the channels in the basins is depicted in Figure 2.5. The following observations are made from the model results:

- The volumes of the channels in the eastern part of the Dutch Wadden Sea (Zoutkamperlaag, Pinkegat and Ameland Inlet) will not change much in the future if the present SLR rate continues. In the western part the channels will decrease their volumes in Vlie and Texel Inlet. This is the continuation of the response to the closure of the Zuiderzee. In the Eierlandse Gat inlet the channel volume will remain increasing due to the increase of the tidal prism.
- Acceleration of SLR causes (relative) increase of the channel volumes. All three scenarios of accelerating SLR cause increases of the channel volumes in all inlet systems except the Texel Inlet. For the Texel Inlet the channel volume will keep decreasing until around 2040 for all scenarios. For the SLR40 scenario this even continues until 2100. It confirms again that there are two factors that influence the development, viz. the SLR rate and the initial state of the system.

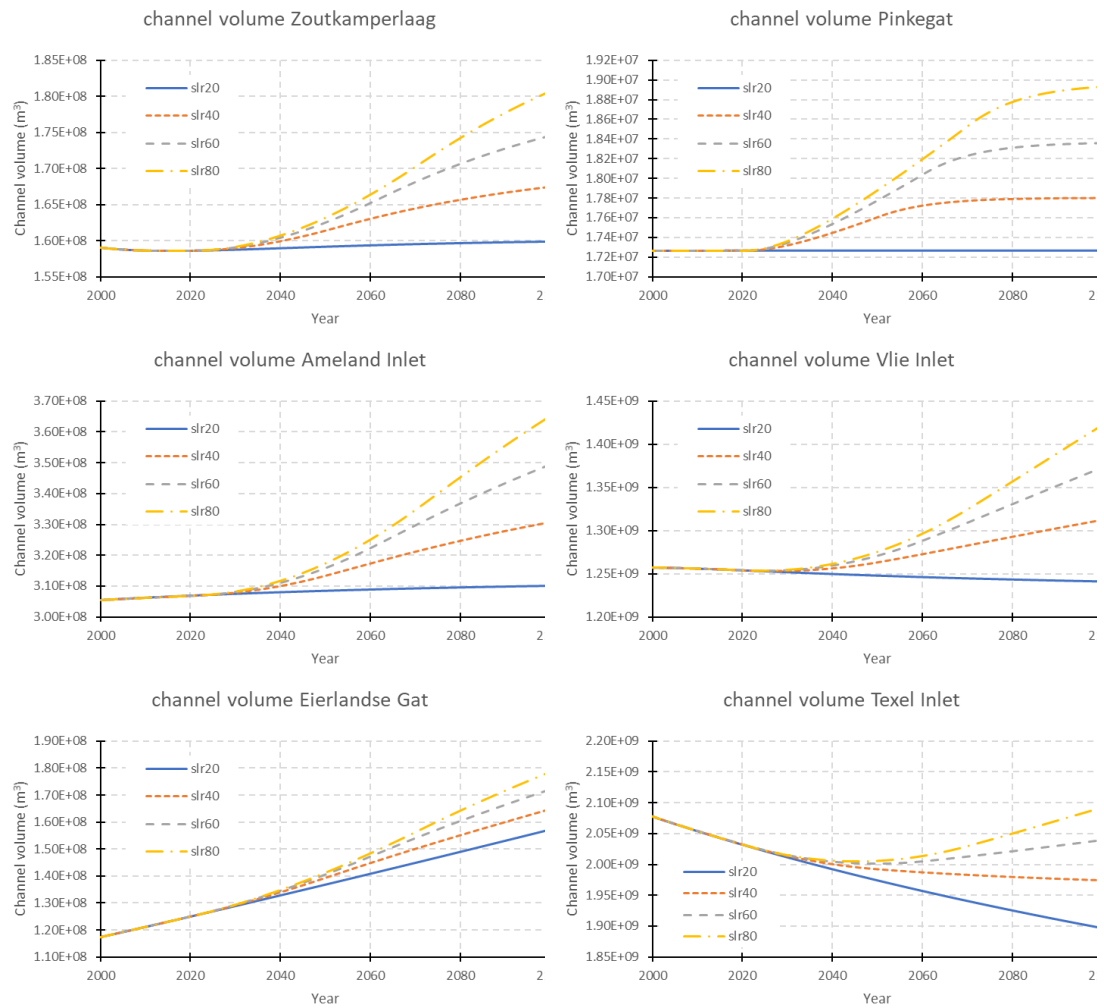


Figure 2.5 Simulated developments of the volumes of the channels in the back-barrier basins.

## 2.6 Development of ebb-tidal deltas

The development of the volumes of the ebb-tidal deltas of the six tidal inlets is shown in Figure 2.6. The models simulate future decrease of the delta volumes for Zoutkamperlaag, Vlie and Texel Inlet, increase for Eierlandse Gat, and practically no change for Pinkegat and Ameland Inlet, if the present SLR rate will continue (SLR20). This behaviour is explained by the initial state, i.e. the continuing influence of the closures of Lauwerszee (Zoutkamperlaag) and Zuiderzee (Texel Inlet and Vlie), and the increase of tidal prism for the Eierlandse Gat. It is further noted that the relative changes of the delta volumes (differences between the different SLR scenarios) are small (all less than 10% of the initial volume) compared to the development of the other elements. There are two reasons for the relative smaller effects. First, the ebb-tidal delta is nearest by the sediment source, the surrounding coastal area (in the model schematised as outside world), so it is easier for this morphological element to achieve dynamic equilibrium. Second, the direct effect of SLR (decreasing the delta volume) and the indirect effect via the change in tidal prism (increasing the equilibrium delta volume) are in opposite direction.

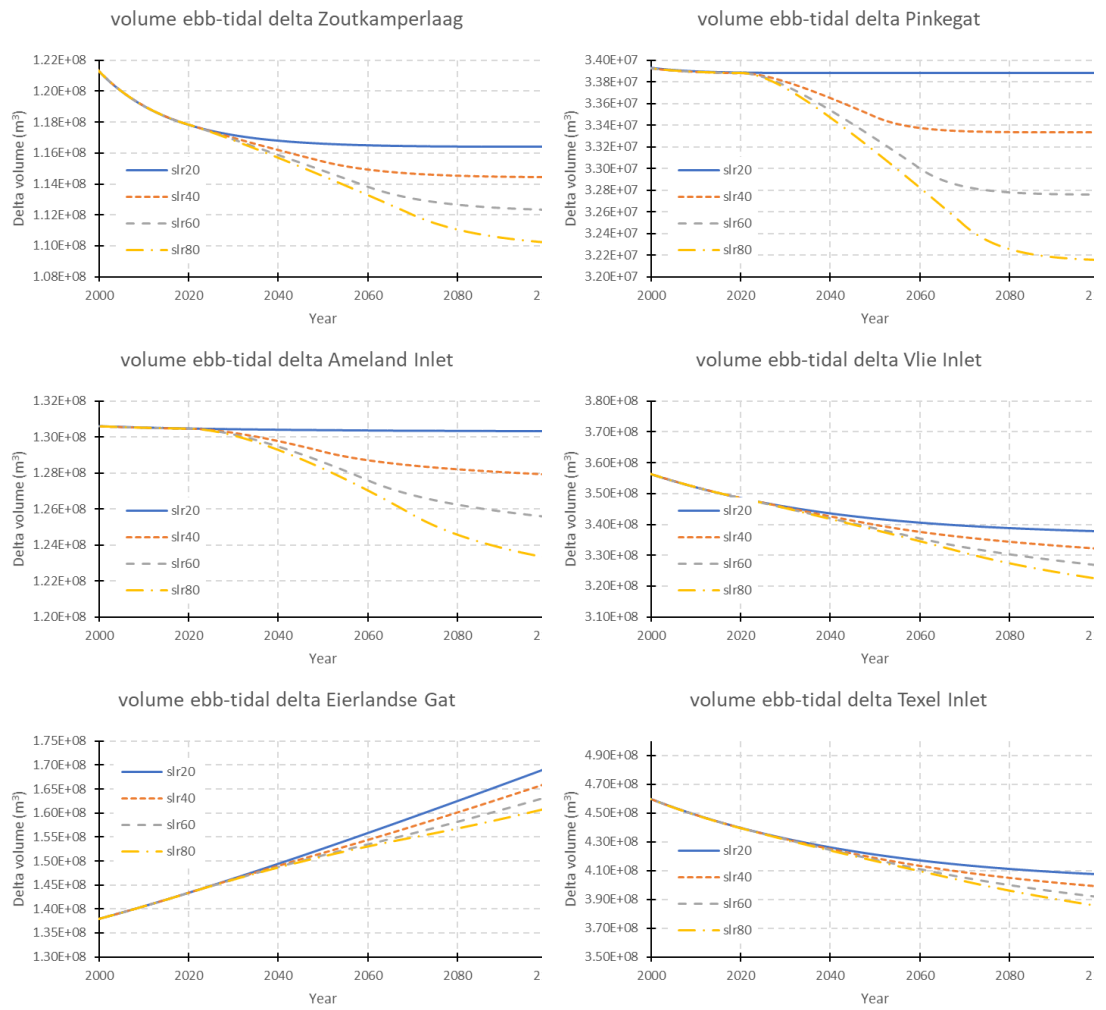


Figure 2.6 Simulated developments of the volumes of the ebb-tidal deltas of the tidal inlets.

# 3 Interpretation of model results for tidal flat development

## 3.1 Introduction

For the ecological functioning of the Wadden Sea, the quantity and quality of the intertidal areas are an important factor. The ASMITA model only describes the impact on intertidal volume. Therefore, in this chapter both a translation of the volume losses to loss in intertidal area and flat height is made by combining the model results with the hypsometric curves (§3.2), as well as an indication of the likely spatial differentiation of changes within each basin, based on understanding of tidal basin evolution under high rates of sea-level rise in the past (§3.3).

## 3.2 Interpretation based on ASMITA simulations

### 3.2.1 Method for translating volume changes to changes in area and average height

ASMITA simulates the volume changes of the morphological elements. However, for the development of the intertidal areas in response to sea level rise, it is relevant to know how the intertidal area and average flat height change. To link the volume changes to changes in area and height, the hypsometric curves from the Wadden Sea inlets are used. A hypsometric curve shows the area proportion of land area that exists at various elevations. Based on the area and elevation occurring between mean low water level (MLW) and mean high water level (MHW), the volume of the intertidal flat can be calculated, and consequently the relation between volume, area and average height (=volume/area) can be derived. Subsequently changes in volume, can also be linked to changes in area and average flat height. This procedure is schematized in Figure 3.1.

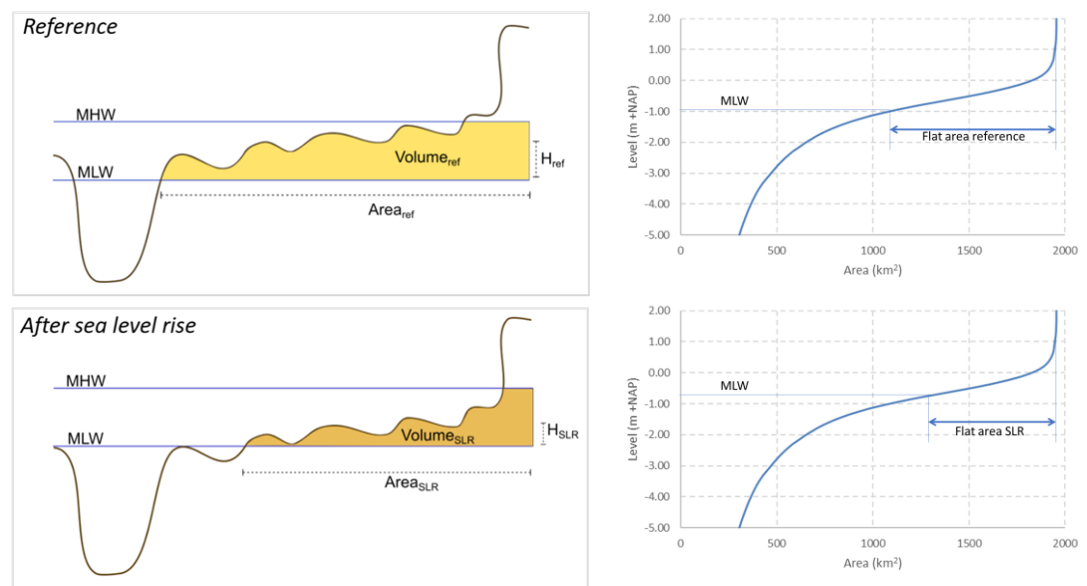


Figure 3.1 Illustration method to derive the relation between tidal flat volume, area and height. The change in volume, area and height is the difference between the values for the reference (top figure) and the situation with sea level rise (bottom figure), left: cross-section, right: hypsometric curve of the Dutch Wadden Sea.

Per definition we have the following relations between the volume  $V_i$ , area  $A_i$  and height  $H_i$  of the intertidal flat in a basin:



$$V_f = A_f H_f \quad (3-1)$$

Note that the flat height is measured from MLW, so it is in fact the averaged thickness of the sediment between MLW and MHW. The calculated change of flat volume is due to two factors, viz. the change of MLW and the morphological change due to sedimentation and erosion. The simulated volume  $\Delta V_f$  change needs to be translated into changes of area  $\Delta A_f$  and height  $\Delta H_f$ . There is thus only one relation for two unknowns.

$$\Delta V_f = A_f \Delta H_f + \Delta A_f H_f + \Delta A_f \Delta H_f \quad (3-2)$$

As shown in Fig.3.1, the distribution to changes in area and height of the volume due to change in MLW can be determined if the shape of the hypsometric curve is known. In this study, this distribution is also applied to the volume change due to sedimentation and erosion. Sedimentation is assumed to be equivalent as a lowering of the MLW and erosion as a rise of MLW.

The values for MLW and MHW are derived from a combination of the mean sea level (MSL) from the “Zeespiegelmonitor 2018” (Baart et al. 2019) and the estimates for the average tidal range, see Table 2.1:

$$\text{MLW} = \text{MSL} - \text{Tidal range}/2; \quad \text{MHW} = \text{MSL} + \text{Tidal range}/2 \quad (3-3)$$

For the translation of volume changes to area and height changes, the last available hypsometric curves are used, see Table 3.1.

Table 3.1 Year of used hypsometric curve per inlet.

Marsdiep	Eierland	Vlie	Ameland	Pinkegat & Zoutkamerperlaag
2009	2011	2010	2012	2012

This method for estimating the changes in area and height assumes that the shape of the hypsometric curve does not change over time, which means that sedimentation, if any, is spread evenly in the intertidal area. This is however not the case as the available hypsometric curves in different years do not have exactly the same shape. To get an indication on how morphodynamic changes may change the relation between volume, area and average height, all available historic hypsometric curves have been included in the analysis (Nederhoff et al., 2017), to derive a band width reflecting historical variations, see Figure 3.2.

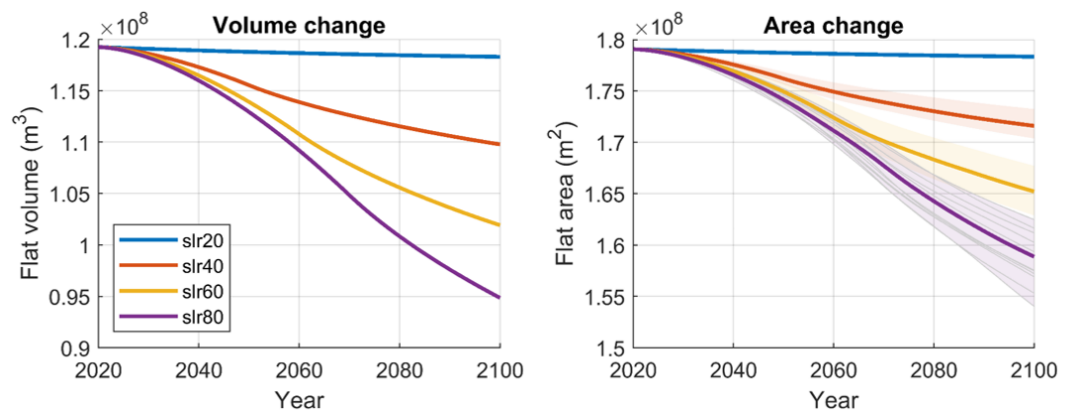


Figure 3.2 Illustration on how changes in area related to a given changes in volume as determined by historic hypsometric curves (grey lines) are converted to band width that reflect the range of historical changes. Left, the calculated volume change and right the related change in area (Amelanderzeegat). Method is illustrated for the slr80 scenario.

Note that the historic variations reflect both natural variations as well as the response of the system to closure of the Zuiderzee, which affected the western inlets. As such the band width cannot be regarded as an uncertainty band, but only reflects a possible variation that may occur for future predictions of change in area or height.

The available hypsometry curves (Nederhoff et al., 2017) from before 2000 show stepwise changes. The reasons for these steps are related to resolution or processing of the data. Prior to estimating the relations between volume, area and height of the intertidal area, these curves have been smoothed with a Gaussian filter. Otherwise artificial steps in area or height changes occur in response to change in volume, see Figure 3.3.

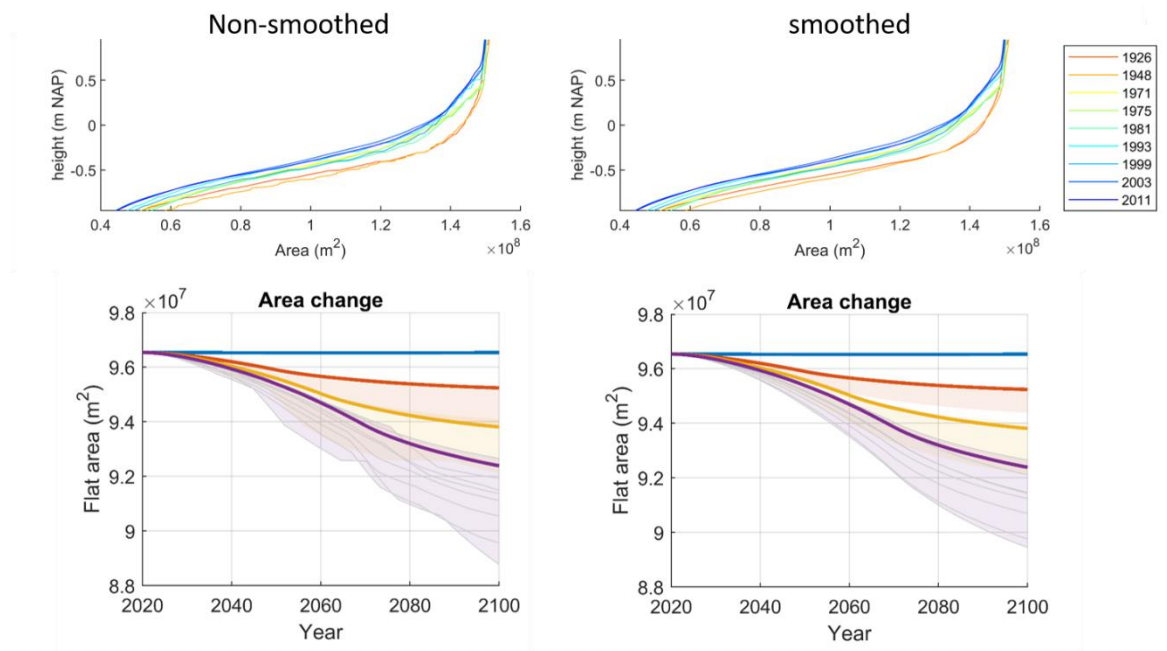


Figure 3.3 Effect smoothing of the hypsometric curves on the prediction of change in area. Note that only in the historic lines (grey lines) have been smoothed.

For determining the intertidal area and volume from each hypsometric curve, first the MLW and MHW have been determined based on formula (3-3). The sea level has been assumed to change according to the values reported in the “Zeespiegelmonitor 2018” (Baart et al. 2009), for Harlingen and Den Helder. Without including the change in historic sea level rise, a larger spread of historic changes in the relation between volume, area and height is observed. In this analysis, only results including historic change in mean sea level are reported.

Note that for Ameland Inlet the bathymetric measurements from before 1970 are less reliable (Elias 2019b) and therefore disregarded. As no separate hypsometric curves are available for the Zoutkamperlaag and Pinkegat, the results for these two inlets are combined.

### 3.2.2 Development of intertidal area and flat height

The changes in tidal area and average flat height in response to sea level rise scenarios SLR20, SLR40, SLR60 and SLR80 are shown in Figure 3.5 to Figure 3.9. The year 2020 is taken as reference, and 2100 as projection. All results are summarized in Table 3.2 and Figure 3.4.

The following observations are made:

- At a sea level rise rate of 2 mm/year, all tidal inlets will be able to keep pace with sea level rise and show no loss of tidal flat in 2100. The tidal volume in the Marsdiep and Vlie inlet will even increase, as sedimentation rate exceeds the rate of sea level rise. This effect is largest for the Marsdiep, with a final increase of 7% in intertidal volume, 6% in area and 2% in average height.
- Simulations suggest that for the three scenarios with accelerating sea level rise, i.e. with sea level rise rate of 4 mm/year or higher in 2100, the sedimentation rate is lower than sea level rise rate, resulting in a loss of intertidal volume, area and height for all inlets.
- The largest change in intertidal volume is expected to occur in the Vlie and Ameland inlet, showing respectively a 23% and 20% loss in 2100 for the slr80 scenario. The loss of intertidal volume, percentage wise results in an equal loss in area and height, of between 11 – 16%. Aside from the largest change in volume, also the largest change in flat height occurs in these two inlets, with a reduction in flat height of 6.6 cm (12%) for the Vlie inlet and 7.6 cm (11%) for the Ameland inlet.
- The smallest change in intertidal volume is expected to occur in the inlets of Pinkegat and Zoutkamperlaag, namely 9% loss in 2100 for the SLR80 scenario. The change in intertidal volume mostly results in a loss in average flat height, namely 5.8 cm (7%), and a relatively small loss of intertidal area of  $2.9 \cdot 10^6 \text{ m}^2$  (2%).
- Medium volume changes occur in the basins of Texel Inlet (Marsdiep) and Eierlandse Gat, with a prognosed loss of respectively 17% and 14% in 2100 for the slr80 scenario. For the Marsdiep the volume change mostly results in loss of area,  $16 \cdot 10^6 \text{ m}^2$  (13%), the change in average flat height stays limited to about 3 cm loss (6%). For Eierlandse Gat, the opposite occurs and the loss in intertidal volume mostly results in a loss of height of 5.3 cm (9%). The loss in intertidal area stays limited to  $4.1 \cdot 10^6 \text{ m}^2$  (4%).

Table 3.2 Overview of changes in flat volume, area and height in 2100, for the different inlets and for the four types of sea level rise rate scenarios. The colours indicate how strong the change is, with highest losses in red and smallest losses or even small gains in green.

	SLR (mm/year)	Volume change (m3)	Area change (m2)	height change (cm)	Volume change	Area change	Height change
Marsdiep	2	4.1E+06	6.7E+06	1.0	7%	6%	2%
	4	-7.3E+05	-1.2E+06	-0.2	-1%	-1%	0%
	6	-5.4E+06	-8.6E+06	-1.4	-9%	-7%	-3%
	8	-9.8E+06	-1.6E+07	-2.8	-17%	-13%	-6%
Eierland	2	-1.2E+04	0.0E+00	0.0	0%	0%	0%
	4	-2.8E+06	-1.3E+06	-1.9	-5%	-1%	-3%
	6	-5.5E+06	-2.7E+06	-3.7	-10%	-3%	-6%
	8	-8.0E+06	-4.1E+06	-5.3	-14%	-4%	-9%
Vlie	2	3.3E+06	3.3E+06	0.5	2%	1%	1%
	4	-1.5E+07	-1.6E+07	-2.1	-7%	-5%	-4%
	6	-3.1E+07	-3.5E+07	-4.7	-16%	-10%	-8%
	8	-4.6E+07	-5.7E+07	-6.6	-23%	-16%	-12%
Ameland	2	-9.5E+05	-7.3E+05	-0.3	-1%	0%	0%
	4	-9.5E+06	-7.5E+06	-2.9	-8%	-4%	-4%
	6	-1.7E+07	-1.4E+07	-5.4	-15%	-8%	-8%
	8	-2.4E+07	-2.0E+07	-7.6	-20%	-11%	-11%
Pinkegat & Zoutkamper- laag	2	-3.4E+05	-1.0E+05	-0.2	0%	0%	0%
	4	-3.5E+06	-1.0E+06	-2.2	-4%	-1%	-3%
	6	-6.4E+06	-2.0E+06	-4.1	-7%	-2%	-5%
	8	-9.1E+06	-2.9E+06	-5.8	-9%	-2%	-7%

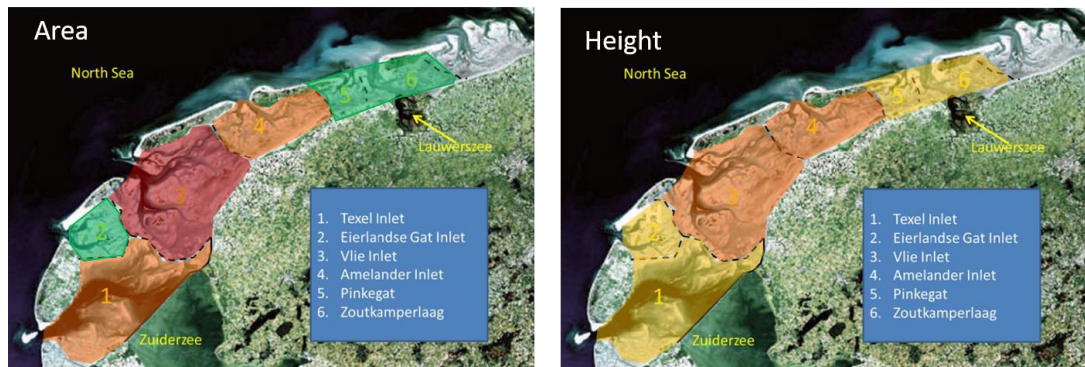


Figure 3.4 Figure summarizing the results, with the changes in area on the left and change in average flat height to the right. The colours indicate how large the losses are, with the largest losses in red (>15% by 2100), the intermediate losses in orange (10%-15%) and yellow (5%-10%) and smallest losses in green (<5%).

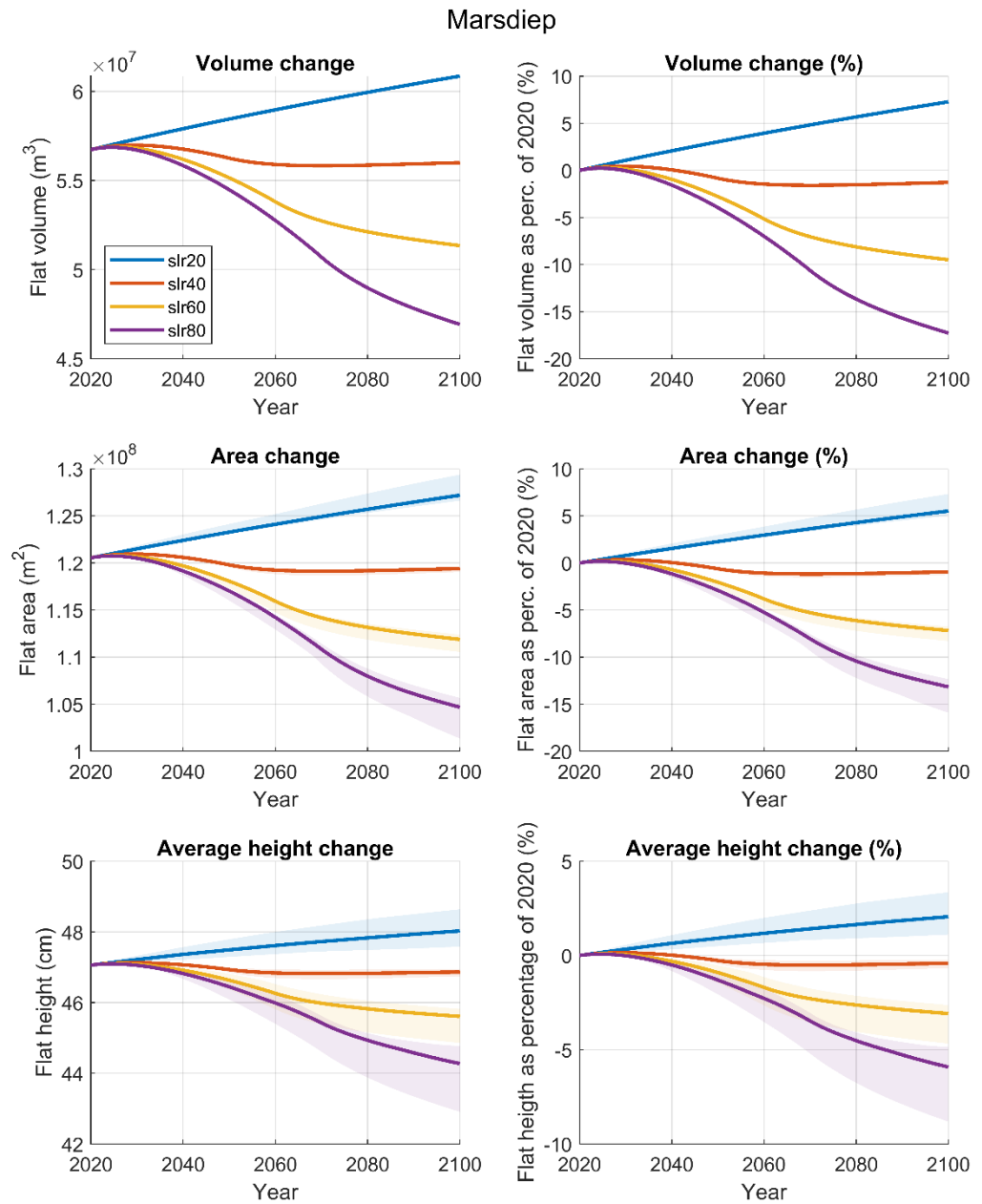


Figure 3.5 Change in volume, area and height for Marsdiep.

Eierland

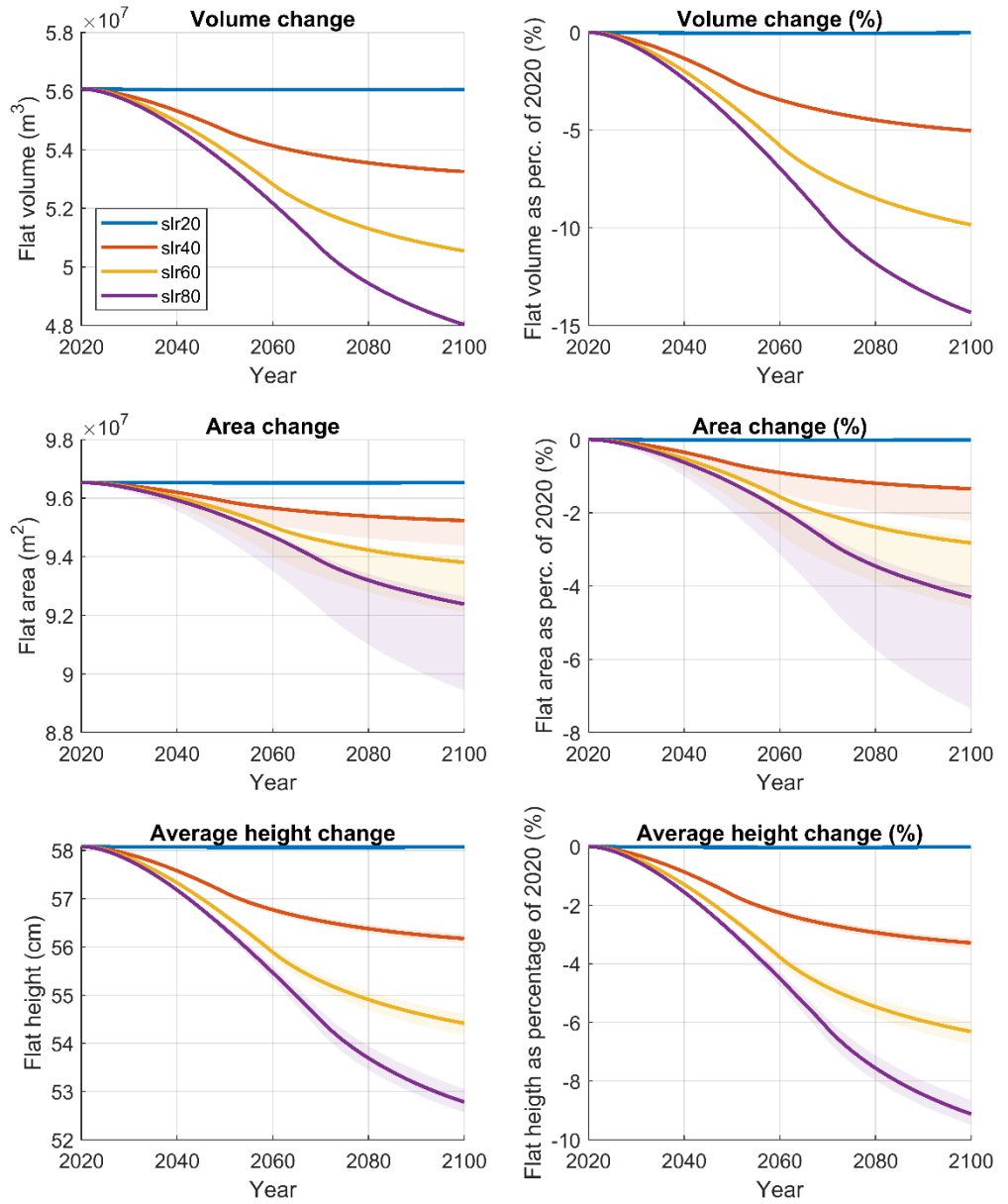


Figure 3.6 Change in volume, area and height for Eierlander inlet.

Vlie

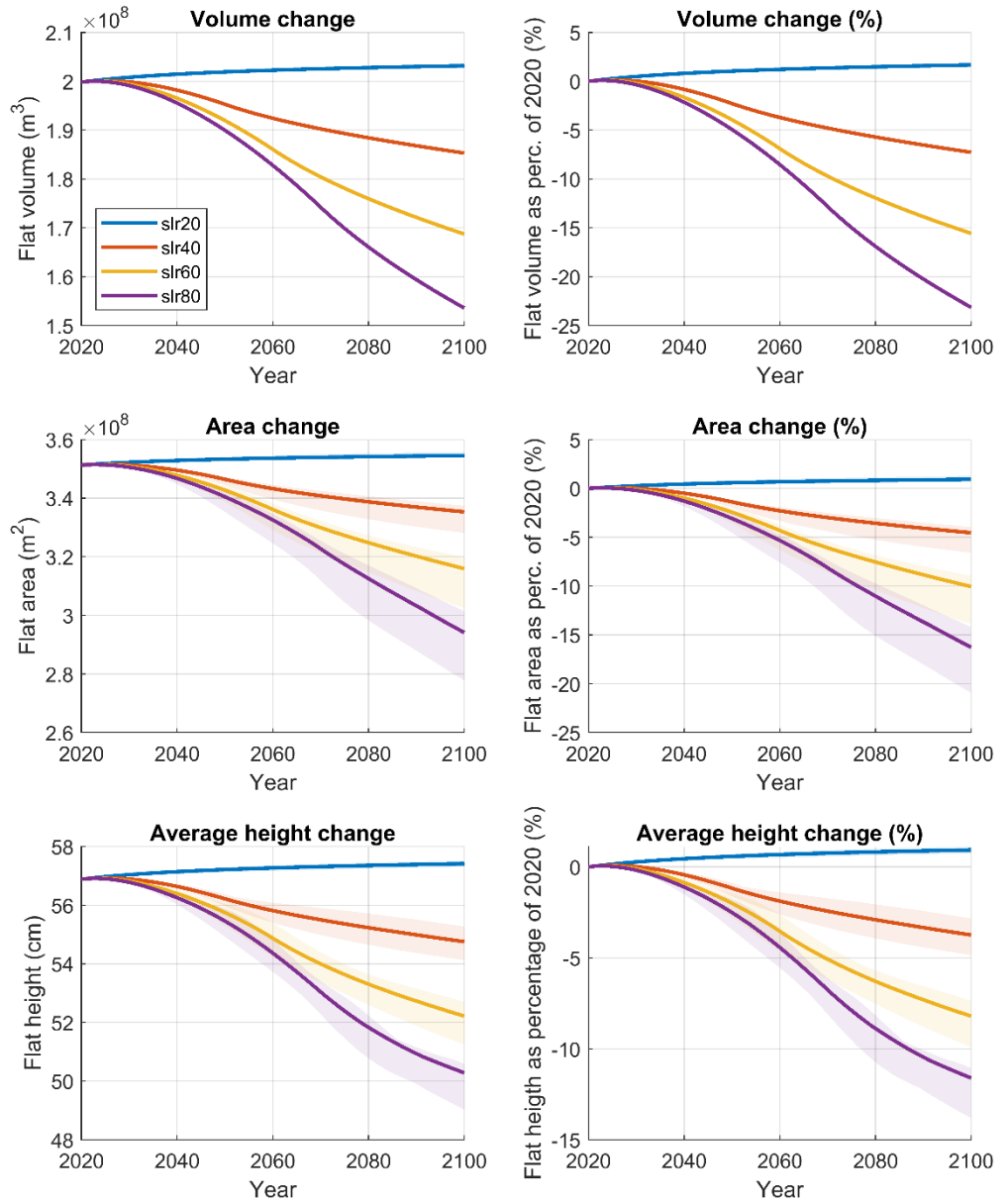


Figure 3.7 Change in volume, area and height for Vlie inlet.

### Amelandzeegat

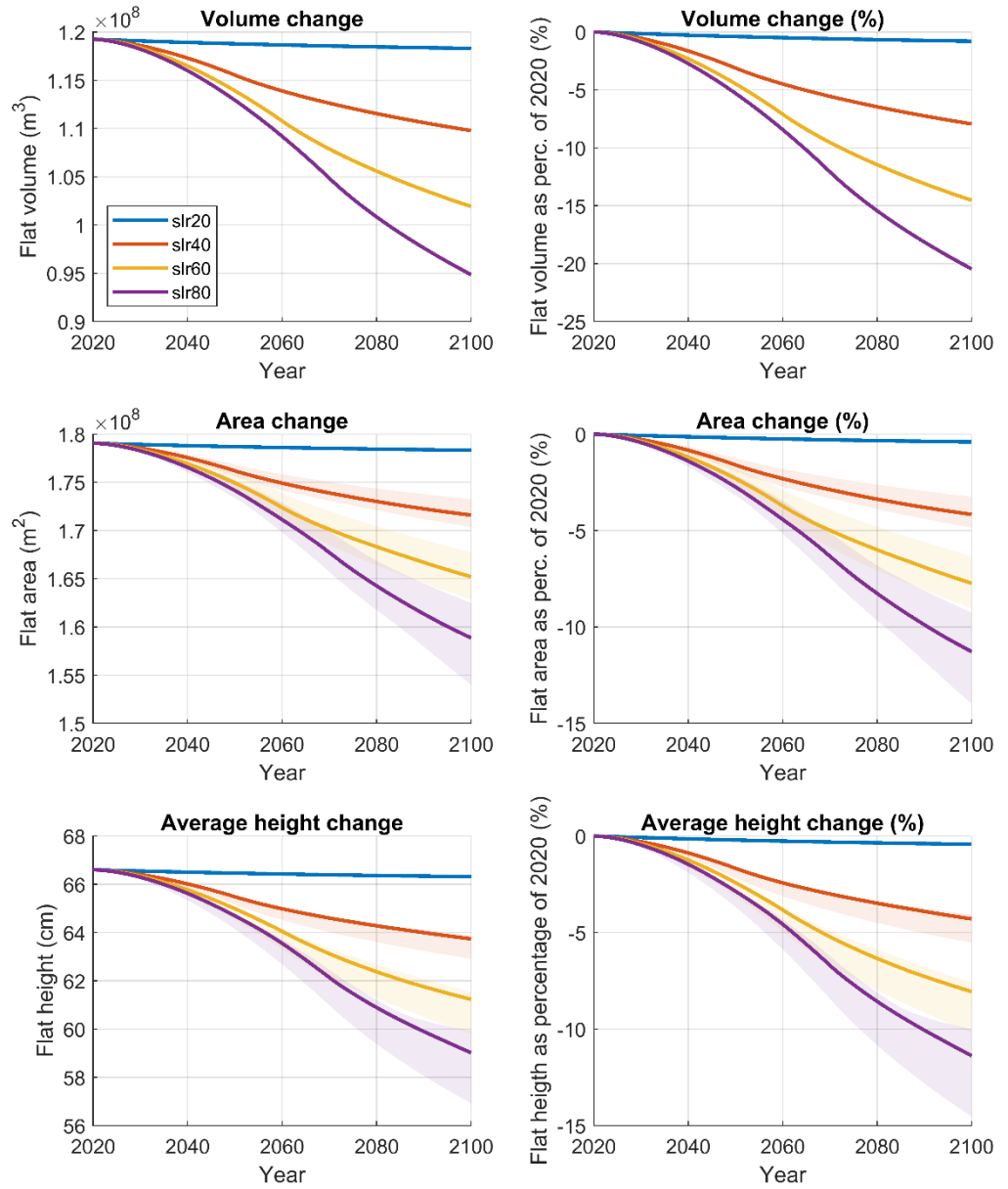


Figure 3.8 Change in volume, area and height for Ameland inlet.



## Pinkegat-en-Zoutkamp

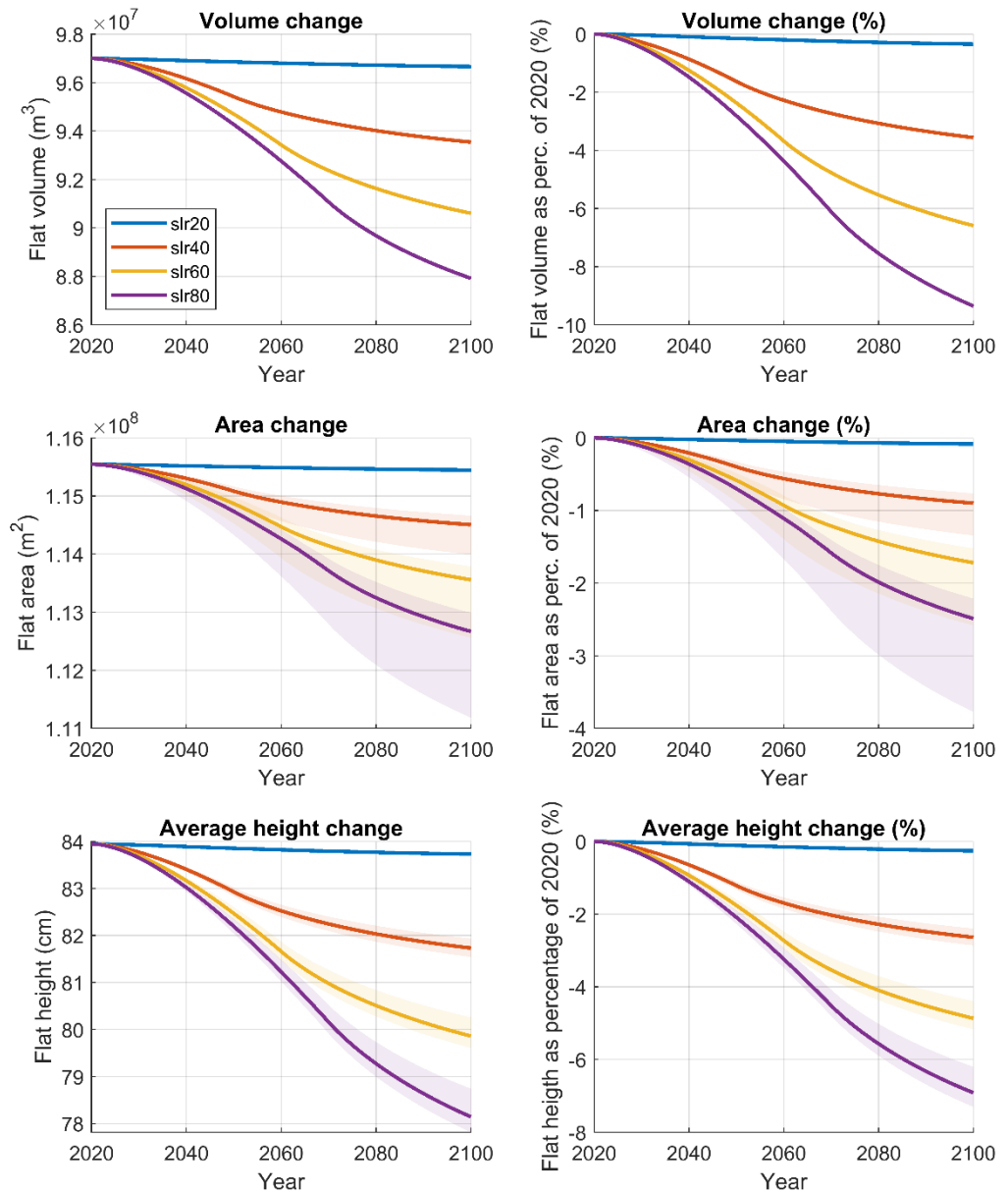


Figure 3.9 Change in volume, area and height for Pinkegat and Zoutkamperlaag

### 3.3 Spatial distribution of tidal flats within the basins

#### 3.3.1 Introduction

The simulated future development of the tidal basins does not give indications of the spatial distribution of intertidal flats in the tidal basins. However, insight into the general principles of sediment supply to, and transport within the basins, enables a reconnaissance of the future developments.

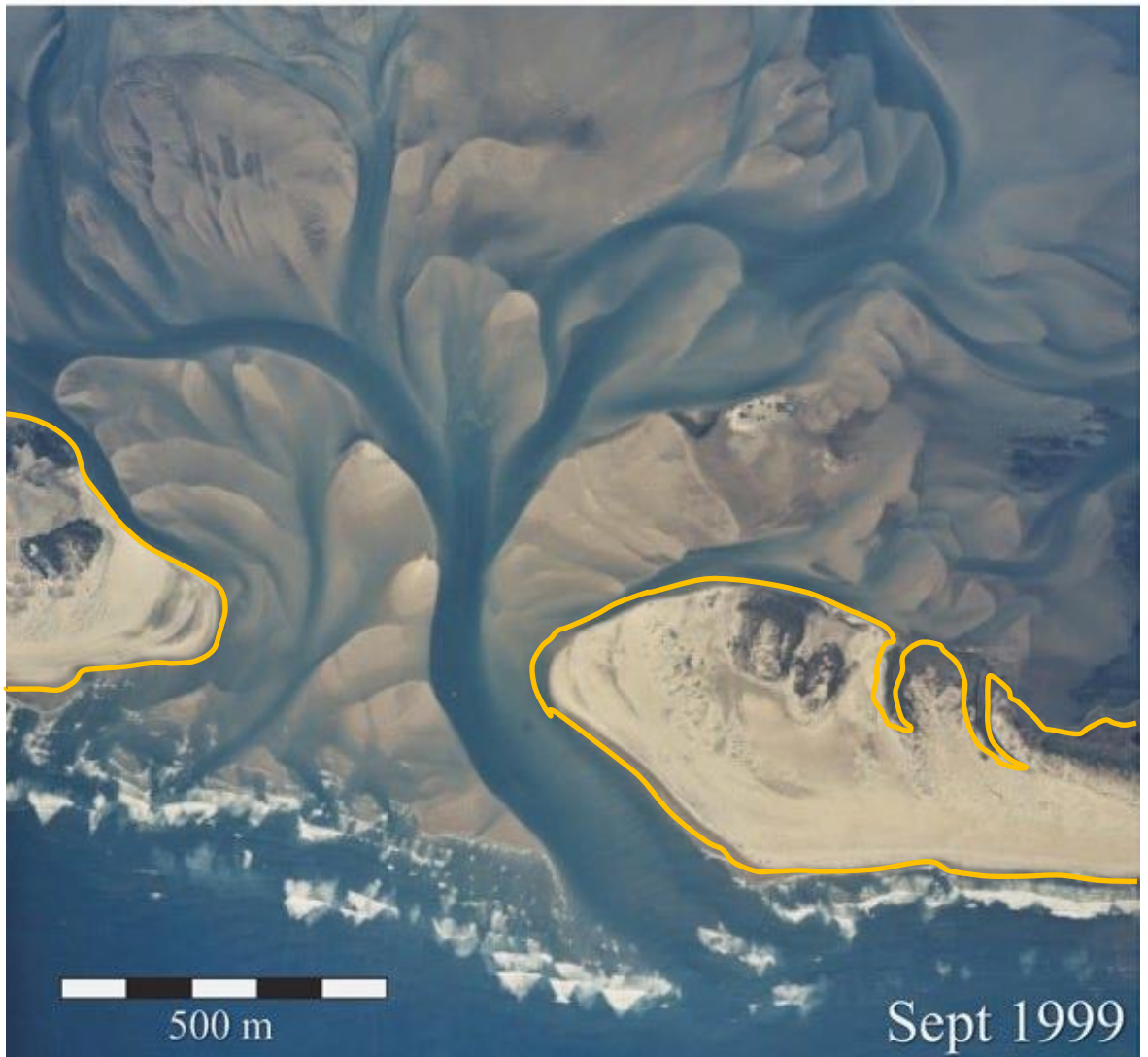


Figure 3.10 Drum Inlet, North Carolina, showing a typical flood-tidal delta. The ocean is on the lower side of the photo. (Photo courtesy Bill Cleary)

### 3.3.2 Pattern of sediment supply and distribution

Sand and mud in the Wadden Sea are supplied by the coastal zone. Erosion of barrier islands, ebb-tidal deltas and the seabed produces sand that is subsequently transported to the inlet and into the basin by tidal currents and wave-driven longshore transport. Ebb currents will bring part of that volume back to the coastal zone. Mud is supplied in suspension and is transported by the net alongshore current from the south and west.

The present-day basins of the eastern Wadden Sea are almost filled with sediment and net accretion is slow. However, if we consider the evolution of a basin from an 'unfilled' stage to a 'filled' stage, we can imagine the formation of a sand body near the inlet fed by the flood transport of sand. Such a sand body is called 'flood-tidal delta' (see Figure 3.10). With time, this delta will grow into the basin until it reaches its boundaries, after which it can only grow vertically.

The present-day eastern Wadden Sea shows the effects of the 'distance to inlet' in its accretion patterns at its tidal watersheds. The tidal watersheds are locations where flood currents coming from 2 directions meet and neutralize each other. Consequently, currents are minimal (except for wind-driven currents) and tidal action is restricted to vertical water motions. Since flood currents arriving from the western inlet arrive earlier than those from the eastern inlet, their meeting point

lies closer to the eastern inlet than to the western. Satellite imagery from this area shows sandy intertidal shoals dissected by meandering channels at the eastern side, in contrast to lower flats dissected by more stable linear channels at the western side. This difference can be contributed to the 'distance to inlet' and the difference in net sand supply and accretion this causes. The migration rate of the channels in the basin shows a similar pattern (Figure 3.11).

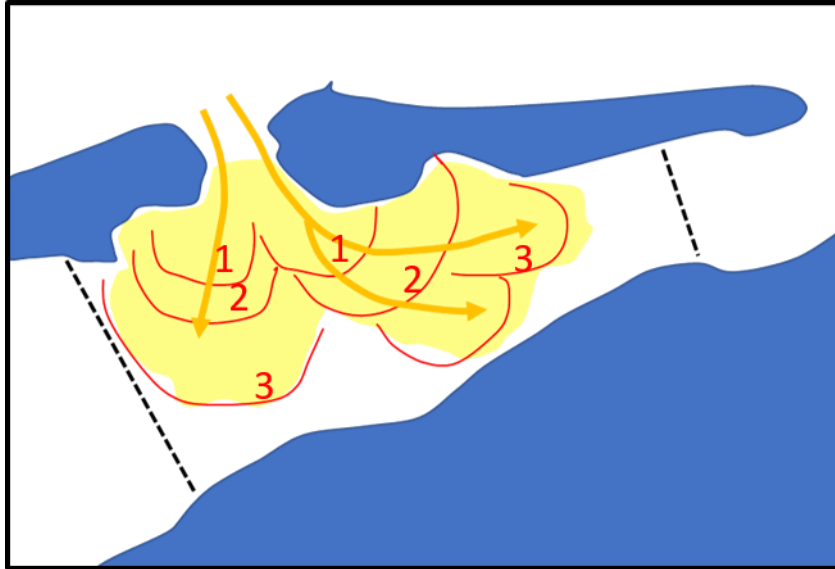


Figure 3.11 Stages of development of a flood-tidal delta within a tidal basin. With infilling of the tidal basin, the delta will grow in surface area, from stage 1 to stage 2 to stage 3, covering an increasing part of the basin area. With a growing sand deficit, the delta will gradually become smaller in reverse order, withdrawing into the direction of the tidal inlet (that conveys the sediment). The area between the flood-tidal delta and the sea dikes/reclamation works will be the first to become subtidal. This area will expand with increasing sediment deficit.

The western Wadden Sea is a different system by origin. Large-scale landscaping processes during the penultimate and ultimate glacial periods created substantial elevation differences in the northern Netherlands. The area that is now the western Wadden Sea has been land until about 2500 year ago. A gradually increasing relative sea-level flooded the area and connected to the large inland-lake Flevo. After that connection the western Wadden Sea rapidly expanded and deep channels scoured the subsurface. High-lying areas remained in between the major tidal inlet-channel systems running south into the lagoon Zuiderzee. Finally, the western Wadden Sea consisted of barrier islands and intertidal flats at its seaward part, resembling a series of flood-tidal deltas, and a large lagoon (or even an estuary, receiving a distributary of the river Rhine) to the south. Because of this evolution, some of the intertidal areas here consist of Pleistocene deposits with a thin veneer of Late-Holocene tidal deposits on top (e.g., Waardgronden, southeast of Vlieland). These areas are dissimilar to the flood-tidal deltas of the eastern Wadden Sea. Besides that, the separation of the Zuiderzee from the western Wadden Sea by the Afsluitdijk triggered large-scale changes in tidal current patterns, sediment transport and morphodynamic evolution.

### 3.3.3 Grain-size selection

Sand is always a mixture of several grainsizes. During transport, selection of grain sizes occurs. The coarsest fractions are transported over or close to the bed and their travelling distance per tide will be small. These fractions are mostly found in the tidal channels. Finer fractions will be transported in suspension in increasing percentages and will thus travel further with the tidal flow. The finer fractions are in general found further into the basin.

Mud is transported into the basin by advection. It will settle in sheltered, quiet locations. Bioaccumulation by filter-feeding benthic organisms produces mud deposits in locations that are not directly governed by physical processes.

Tidal basins in their original state were running perpendicular to the coast since they were drowned valleys draining small-scale rivers and creeks. With the rising sea level following the last ice age, these basins expanded landward. In this configuration, mud deposition occurred predominantly in the sheltered, most landward parts of the basin. After changing into salt marshes and accretion to supratidal level, these areas were protected with (small-scale) dikes and changed into polders. This way, the landward parts of the basins disappeared, gradually reducing the surface area fit for mud deposition. In the present-day situation, large-scale permanent mud deposition has become unlikely without artificial measures such as reclamation works that are designed to reduce wave- and current energy and thus stimulate mud accretion.

#### 3.3.4 Basin morphology under increasing sediment demand

We can apply the described pattern of sediment supply and distribution to future situations. An acceleration of sea-level rise will increase the room for sediment deposition ('accommodation space') in the basins. If the available sand volume in the coastal zone and the transport capacity to carry the sand into the basin remain adequate, the probability of net changes in the sediment balance of the basin is small. However, in case the sand supply to the basin starts to run behind the growth of accommodation space, the basin will undergo a reverse evolution. Vertical accretion will diminish, and the rims of the flood delta will receive gradually less sand. With an increasing sand deficit these rims will gradually disappear under water and the flood delta starts shrinking (see Figure 3.11). The intertidal shoals in the vicinity of the inlet will remain intertidal but the shoals further away will gradually disappear with increasing sediment deficit. A basin lay-out with a flood-tidal delta near the inlet and a subtidal area surrounding it will possibly accumulate more suspended mud in its growing lagoon. Whether the mud will settle and accrete depends on the energy conditions in the basin. The sketched situation resembles the overall morphology of the transgressive Mid-Holocene Holland tidal basin in the western Netherlands. This basin was formed by transgression of the North Sea. The rapid landward expansion of the basin created a large sediment demand that could not be met. Hence, the coastline was constantly moving landwards, and the imported sand was deposited along the tidal channels near the inlets, forming flood tidal deltas (Figure 3.12). The lagoon accumulated mud. See Van der Spek & Beets (1992) for a more detailed description of this setting.

### 3.4 Summary

Based on the Asmita simulations a loss of intertidal area is predicted for all accelerated sea level rise scenarios (SLR40 - SLR80). The largest loss in intertidal volume is expected to occur in the Vlie and Ameland inlet (respectively 23% and 20% loss in 2100 for the SLR80 scenario), the smallest loss is expected to occur in the inlets of Pinkegat and Zoutkamperlaag (9% volume loss in 2100 for the SLR80 scenario). It differs per inlet whether the volume loss mostly results in loss in flat area (inlets of Texel and Vlie) or in average flat height (Pinkegat, Zoutkamperlaag and Eierlandse Gat). Based on the simulations no spatial differentiation can be made. To get an idea on how the loss of intertidal area is distributed within each inlet, the understanding of tidal basin evolution under high rates of sea-level rise in the past is used to sketch the situation to be expected in case the sediment budget becomes negative (§3.3). This shows that a tidal basin with a decreasing sediment supply will start to develop a subtidal lagoon just off the land reclamation works and along the western part of each the tidal watershed. Hence, these are the most vulnerable parts for drowning of tidal flats. With increasing deficit, the flood-tidal delta will gradually draw back to the inlet and the lagoon will expand.

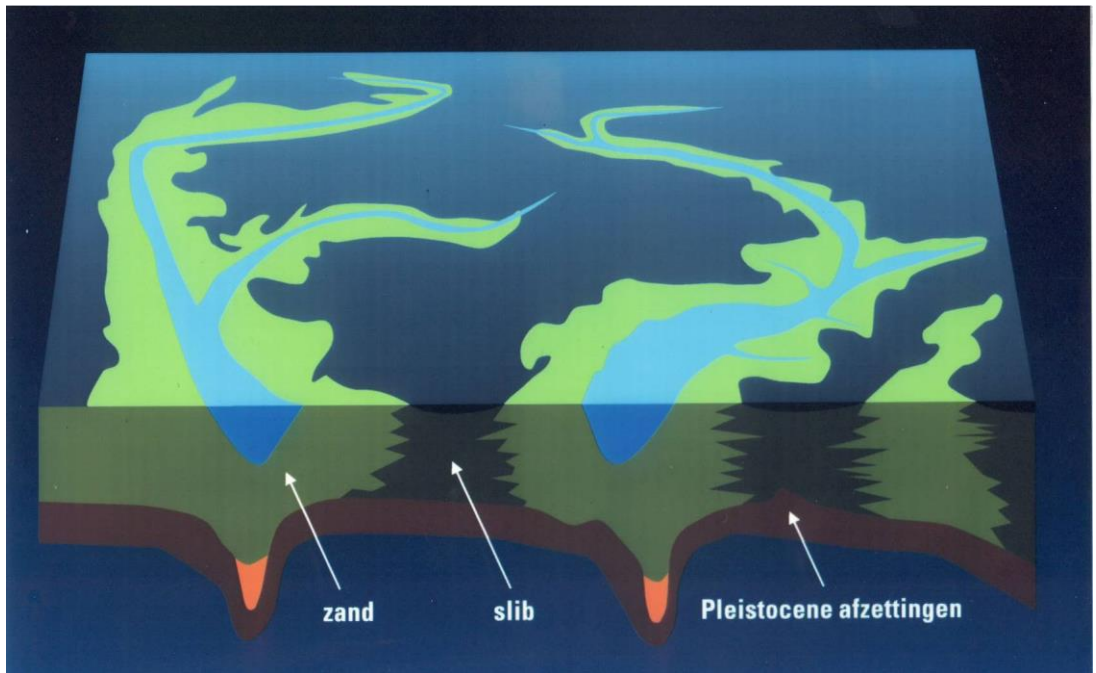


Figure 3.12 Reconstruction of the landward part of a flood-tidal delta in a transgressive tidal basin, looking landward. Sandy tidal flats are bounding the tidal channels. The shallow lagoon in between and landward of the sandy shoals accumulates mud. Based on data from Van der Spek & Beets (1992).

## 4 Discussions

### 4.1 The analyzed ASMITA simulations

Two sets of ASMITA simulations have been presented by Wang and Lodder (2019), one carried out with the then existing ASMITA models, and the other with the updated models. In this study only the second set of simulations, carried out with the updated models, are analyzed and presented. The updates for the ASMITA models were based on the comparison between the hindcasting results and the newest insights from the analysis of historical development (Elias, 2019). For three tidal inlet systems, Vlie, Eierlandse Gat and Texel Inlet, the models have been updated.

It is noted that the updates were meant to improve the reproduction of the sediment exchanges through the inlets, whereas the developments of the individual morphological elements in the tidal inlet systems were not considered. The models are thus not calibrated with the up to date field data concerning the development of the intertidal flats in the Wadden Sea. This has the consequence that there is a discrepancy between the model results (of e.g. tidal flat volume) and observations. The discrepancy has two sources. First, the model schematizations based on the 1970 data were made in the end of last century. The used internal boundaries between the basins of the neighbouring tidal inlets, i.e. the positions of the tidal divides, are not the same as those used in the recent data analyzes (Elias et al., 2012; Nederhoff et al., 2017; Wang et al., 2018; Elias, 2019). Second, there are differences in morphological changes between 1970 – 2020 in the model run and reality (2020 is the reference year for the analysis). However, this shortcoming of the model is expected not to influence the predicted development of the areas and heights of the intertidal flats significantly. The error due to the shortcoming is estimated to be less than the uncertainty induced by using the hypsometric curves from different years.

Wang and Lodder (2018) only updated the model parameters for defining the morphological equilibrium. The parameters influencing the morphological time scales were not updated, although they do influence the simulated response to accelerating SLR. Lodder et al. (2019) shows that especially the power  $n$  in the relation between equilibrium sediment concentration and morphological state can have substantial influence. However, updating this parameter would require an extension of the model to mixed sediment, as it is dependent on the type of sediment. Therefore, this is considered as recommended future work.

The simulations were carried out for the period 1970-2100, and only the forecasting results from 2020 to 2100 are analyzed. According to the simulations, none of the tidal basins will completely drown (defined as: all intertidal flats lost/permanently inundated) in 2100, even though the sea level rise rate of 8 mm/y in the SLR80 scenario exceeds the critical rates for the inlets Texel and Vlie (Wang and Lodder, 2019). The simulated period is simply too short to illustrate the whole drowning process. However, the model results do provide insights on the impact of acceleration of sea level rise on the development of the tidal flats in the Wadden Sea, especially concerning the difference between future and present, e.g. relative loss of flat area in 2100, and the differences between the sea-level rise scenarios.

### 4.2 Model results

Four future SLR scenarios are considered in this modelling study. One with a stable rate of 2 mm/year (current rate), and three scenario's with accelerated sea level rise rates, increasing from current rate of 2 mm/year to 4, 6 and 8 mm/year. Resulting sea level rise between 2020 and 2100 is respectively 16 cm, 29 cm, 40 cm and 49 cm. For the time process of how the SLR is changing from the present rate to the rate in 2100 reference is made to the scenarios described by

Vermeersen et al. (2018). In all four scenarios, the SLR is constant and equal to 2 mm/y until 2020. In the three accelerating scenarios the SLR rate increases linearly in time, starting in 2020 to the maximum value. The increasing period to achieve the 2100 value is until 2050 for the 4 mm/y scenario, until 2060 for the 6 mm/y scenario and until 2070 for the 8 mm/y scenario. Four scenarios are simulated with the updated ASMITA models for the six tidal inlet systems: Zoutkamperlaag, Pinkegat, Ameland Inlet, Vlie, Eierlandse Gat and Texel Inlet.

The differences in SLR between the four scenarios start in 2020, resulting in corresponding differences in the development of the tidal flat between the scenarios. No delay in response is observed. This contrasts with the differences in the simulated sediment transport through the inlets that do show a delay in response of decades (Wang and Lodder, 2019). The immediate response of the development of the tidal flats and the delayed response of the sediment transport through the inlets are in fact related. The delay in sediment transport means also delay in sedimentation on the tidal flats, so the tidal flats reduce in area and height immediately if more sea level rise occurs. The development of the intertidal flats in the Wadden Sea is thus sensitive to the sea level rise scenario.

The tidal basins in the Wadden Sea will respond differently when SLR accelerates. The SLR rate will be the same but the critical SLR rate for drowning is very different between the basins. In Table 4.1 the critical SLR rates for the six tidal basins in the Dutch Wadden Sea, as calculated by Wang et al. (2018) are given together with the dimensionless SLR rate  $r$  (SLR rate divided by the critical rate) for four SLR rates (2, 4, 6 and 8 mm/y). The dimensionless SLR rate determines the behavior of a tidal basin concerning the dynamic morphological equilibrium as well as the morphological timescale for achieving the dynamic equilibrium according to the theoretical analysis (Wang and Lodder, 2019). The delay of sedimentation on the tidal flats depends on the morphological timescales, so it is smaller for the smaller inlet systems than for the larger systems. The delay depends also on present state of the system concerning in how far the system is deviated from the (dynamic) morphological equilibrium, so it e.g. becomes very large for the Texel Inlet with a large existing sediment demand.

Table 4.1. Critical SLR rate for drowning of the various tidal inlet systems in the Dutch Wadden Sea from Wang et al. (2018) and the dimensionless SLR rate  $r$  for four different SLR rates (2, 4, 6 and 8 mm/y).

Inlet	$R_c$ (mm/y)	$r$ for SLR rate =			
		2 mm/y	4 mm/y	6 mm/y	8 mm/y
Texel	7.00	0.29	0.57	0.86	1.14
ELGT	18.0	0.11	0.22	0.33	0.44
Vlie	6.30	0.32	0.63	0.95	1.27
Amel	10.4	0.19	0.38	0.58	0.77
PinkeG	32.7	0.06	0.12	0.18	0.24
ZoutK	17.1	0.12	0.23	0.35	0.47

If the future SLR rate remains unchanged (SLR20 scenario), the model results predict practically no change of the intertidal flats in the Wadden Sea basins. Only in the two large basins in the western part, Marsdiep and Vlie, a small increase of the intertidal flat is predicted. For all three scenarios of accelerating SLR a loss of intertidal flats in all basins is predicted. The predicted loss is the largest in the two larger basins in the western part, Marsdiep (13% area loss in 2100 for SLR80 scenario) and Vlie (16% area loss in 2100 for SLR80 scenario).

It is remarkable that the loss in the much smaller Ameland basin is also relatively large (11% area loss in 2100 for SLR80 scenario). This agrees with the conceptual model of Wang et al. (2018) that the sediment import (thus also sedimentation in the basin) is limited by accommodation space, implying a relatively larger delay in the response to SLR change.

In the smaller basins, Eierlandse Gat, Pinkegat and Zoutkamperlaag, the effects of SLR acceleration on the area of intertidal flats are much less and hardly noticeable (<5%) according to the model results. However, the effects of the averaged height of the intertidal flats are more noticeable (up to almost 10%), see Table 3.2.

The difference in the distribution of the intertidal flat volume change to area change and averaged height change between larger basins and smaller basins is remarkable. In the larger basins (Marsdiep and Vlie) the volume changes mainly result in area changes. In the smaller basins (Eierlandsegat, Pinkegat and Zoutkamperlaag) the volume changes mainly result in height changes. This distribution is determined by the shape of the hypsometric curves. For Ameland Inlet the volume change is equally distributed to changes in area and height.

The model does not spatially differentiate within each basin. To get an idea on where the largest losses of intertidal area may occur, a system analysis of the Holocene tidal basin evolution is carried out. This suggests that a tidal basin with a decreasing sediment supply will start to develop a subtidal lagoon just off the land reclamation works and along the western part of the tidal watershed. Hence, these are the most vulnerable parts for drowning of tidal flats. With increasing deficit, the flood-tidal delta will gradually draw back to the inlet and the lagoon will expand.

The model results also provide information on the development of the other morphological elements in the tidal inlet systems, the channels in the basins and the ebb-tidal deltas, although they are less analyzed in the present study (see Chapter 2).

The predicted losses of intertidal area are slightly less than those predicted by Wang et al. (2018), although a direct comparison between the two studies is not straightforward because of difference in SLR scenarios considered. The SLR80 scenario in the present study is between the RCP4.5 (SLR rate in 2100 equal to 6.6 mm/y) and RCP8.5 (11.9 mm/y in 2100) scenarios considered by Wang et al. (2018). The present study predicts a loss of the total area of intertidal flats in the Dutch Wadden Sea of about 12% in 2100 (Table 3.2) for the SLR80 scenario. This is close to the loss according to the projection by Wang et al. (2018) for the RCP4.5 scenario (13%) and far less than that for the RCP8.5 scenario (38%). It is understandable that the projection of Wang et al. (2018) is more pessimistic as it assumes that the sedimentation rate in the Wadden Sea will not change in the future and remain the same for all SLR scenarios.

## 4.3 Uncertainties

There are various sources of uncertainties in the presented model results. First and as already mentioned, the models have not been extensively calibrated for reproducing the development since 1970. However, Wang and Lodder (2019) have shown that this has practically no effect on the model results concerning e.g. the differences between the SLR scenarios.

A major uncertainty concerns the SLR development itself, as indicated by the four very different scenarios. In contrast to the sediment transport through the inlets the development of the tidal flat is very sensitive to the sea-level rise scenarios. For the future ecological functioning of the Wadden Sea the uncertain development of SLR is the major source of uncertainty.

The remaining source of uncertainties is due to the shortcomings of the models. This source of uncertainty has been discussed by Wang and Lodder (2019). Their discussions were related to



the sediment transport through the inlet, but the conclusions remain applicable for the development of the intertidal flats.

In Chapter 3, an indication of the uncertainties in the predictions is given, by translating the volume changes to changes of area and height of intertidal flats using hypsometric curves from different years.

# 5 Conclusions and recommendations

## 5.1 Conclusions for management

In addition to the conclusions concerning the sediment transport through the inlets given by Wang and Lodder (2019), the following conclusions are relevant for the management of the Wadden Sea:

- The effect of SLR acceleration on the loss of intertidal flats will be noticeable earlier than the effect on the sediment import rates into the Wadden Sea (thus loss from the coast). The delayed response of the sediment import means a direct decrease in the areas and relative heights of the intertidal flats in the Wadden Sea.
- The development of the intertidal flats is sensitive to the SLR scenarios, while the sediment import in the Wadden Sea is less sensitive to the SLR scenarios. Better prediction of the future SLR development is thus very important concerning the ecological system of the Wadden Sea.
- Acceleration of SLR will affect the intertidal flats in the Wadden Sea, decreasing their horizontal area and their relative height. For the whole Dutch Wadden Sea, the highest SLR scenario (SLR80) used in this study will result in an area loss of about 12% in 2100. Largest losses are predicted for the two larger basins in the western part, with 13% area loss in the Marsdiep and 16% area loss in the Vlie. Considering the uncertainties of the results we conclude that the loss of intertidal area will be less than 20% in 2100 for the considered SLR scenarios.
- Within a tidal basin the effect of accelerated SLR will be most noticeable at the inner edge of the flood-tidal delta, the area between the tidal inlet and the mainland coast.

## 5.2 Recommendations

Concerning **management of the Wadden Sea system** the following recommendations made by Wang and Lodder (2019) are also relevant concerning the development of the intertidal flats in the Wadden Sea:

- Study whether nourishment strategies can significantly influence the sediment import into the Wadden Sea. Given the uncertain future development of SLR and the different (maybe even conflicting) effects of sediment import on coastal maintenance and conservation of ecological value in the Wadden Sea, it is desirable to be able to influence the import rates through the inlets. A possibility to be considered is to apply nourishments on e.g. the ebb-tidal deltas.
- Combine field observation with modelling for monitoring effects of (changing) SLR on the development of tidal flats. Development of SLR itself can be well monitored via field measurements, but combination with modelling will be needed to conclude if certain limit (for e.g. drowning of tidal flats) will be exceeded.

Recommendations concerning **research to the Wadden Sea system in general**, as already made by Wang and Lodder (2019):

- More emphasis on the determination of import rates through the various tidal inlets by combining data analysis and modelling of hydrodynamic and sediment transport processes is recommended. The present rate of import to the Wadden Sea will be a good prediction for a long time (decades) in the future and it is the main uncertain part in the development.
- Investigate the development of the tidal divide areas in the Wadden Sea. In the ASMITA modelling the tidal inlets are considered as isolated systems, assuming that the tidal divides

form the closed boundary between the tidal basins. Whether this assumption is justified depends on the development of the tidal divides responding to the changing SLR.

- Investigate the development of the tidal range in the tidal basins in relation to the morphological changes. According to the model results, the development of the sediment exchange between the North Sea coasts and the Wadden Sea is sensitive to the development of the tidal range in the Wadden Sea. In the ASMITA modelling the change of the tidal range corresponding to SLR and morphological development is not taken into account. Therefore, the investigation needs to be carried out with data analysis for the past, and with process-based models for the future.
- Investigate expected dynamic equilibrium states for all Wadden Sea basins.
- Investigate the effect of sediment distribution on the import rate and tidal flat accretion. The availabilities of different sediment fractions will influence the accretion of the different parts in a basin.

In addition, it is recommended to make the internal distribution of the loss of intertidal flats, as conceptually described in Section 3.2, more specific per basin.

Concerning **ASMITA modelling**, the following recommendations were already made by Wang and Lodder (2019):

- Improving ASMITA by implementing graded sediment transport module, at least by including a sand and a mud fraction. This is important for better prediction of the critical SLR rate for drowning as indicated by the theoretical analysis, and also important for understanding the behavior of the tidal inlet systems responding to accelerating SLR determined by the dimensionless SLR rate.
- Extend the ASMITA models for the tidal inlet systems by including a saltmarsh in the back-barrier basin as an additional morphological element. This is especially important after improving ASMITA with a mud transport.
- Extend the present three-elements schematization of the ASMITA models by dividing the basins into more subparts, based on e.g. the insights from the analysis of Elias (2019). Most important thing for this extension is the applicability of the empirical relations for the morphological equilibrium for the subparts of the basins.
- Combine with process-based modelling for e.g. better setting for the parameters influencing the morphological timescales.

In addition, the following recommendations are made:

- Extend the simulation period. The analysed simulations were carried out until 2100. This simulation period is relatively short compared to the relevant time scales. Even for the cases that the critical SLR rate is exceeded, the drowning process in the corresponding basins cannot be investigated with the existing simulations because of the too short simulation period.

Carry out simulations for more severe SLR scenarios in order to investigate the drowning processes of the intertidal flats in the Wadden Sea basins.

## 6 References

- Baart, F., Rongen, G., Hijma, M.P., Kooi, H., De Winter, R., & Nicolai, R.. 2019. "Zeespiegelmonitor 2018 - De Stand van Zaken Rond de Zeespiegelstijging Langs de Nederlandse Kust." 11202193-000-ZKS-0004. Delft: Deltares.
- Elias, E.P.L., Van der Spek, A.J.F., Wang, Z.B. & De Ronde, J.G., 2012. Morphodynamic development and sediment budget of the Dutch Wadden Sea over the last century. *Netherlands Journal of Geoscience* 91: 293-310.
- Elias, E.P.L., 2018, Rapport data analyse westelijk deel NL Waddenzee.
- Elias, E.P.L., 2019a, Rapport data analyse oostelijk deel NL Waddenzee.
- Elias, E.P.L. 2019b. Een actuele sedimentbalans van de Waddenzee. Deltares rapport, 11203683-001-ZKS-0002, Deltares, Delft, 83p.
- Lodder, Q.J. Wang, Z.B., Elias, E.P.L., van der Spek, A.J.F., de Looft, H., Townend, I.H., 2019, Future Response of the Wadden Sea Tidal Basins to Relative Sea-Level rise—An Aggregated Modelling Approach, *Water* 2019, 11, 2198; doi:10.3390/w11102198.
- Nederhoff, K., Smits, B. & Wang, Z.B., 2017. KPP Wadden, Data analyse: getij en morfologie. Report 11200521-000-ZKS-0002, Deltares (Delft).
- Stive M J F and Wang Z B, 2003, Morphodynamic modelling of tidal basins and coastal inlets, In: *Advances in coastal modelling, Series, Vol, Lakkhan C (ed), pp. 367-392, Elsevier Sciences, Amsterdam.*
- Van der Spek, A.J.F., & D.J. Beets, 1992. Mid-Holocene evolution of a tidal basin in the western Netherlands: a model for future changes in the northern Netherlands under conditions of accelerated sea-level rise? In: J.F. Donoghue, R.A. Davis, C.H. Fletcher & J.R. Suter (eds.), *Quaternary Coastal Evolution. Sedimentary Geology* 80: 185-197.
- Van Goor M A, Zitman T J, Wang Z B and Stive M J F, 2003, Impact of sea-level rise on the morphological equilibrium state of tidal inlets. *Marine Geology*, 202, 211-227.
- Vermeersen, L.L.A., Slangen, A.B.A. et al., 2018. Sea level change in the Dutch Wadden Sea. *Netherlands Journal of Geoscience, Netherlands Journal of Geosciences*, 97-3: 79-127.
- Wang, Z.B., Steetzel, H. en M. van Koningsveld, 2006, Effecten van verschillende scenarios van kustonderhoud, Resultaten lange-termijn simulaties morfologische ontwikkeling Nederlandse Noordzeekust, WL | Delft Hydraulics, Rapport Z4051.
- Wang, Z.B., Elias, E.P.L., Van der Spek, A.J.F. & Lodder, Q.L., 2018. Sediment budget and morphological development of the Dutch Wadden Sea - impact of accelerated sea-level rise and subsidence until 2100. *Netherlands Journal of Geosciences*, 97-3: 183-214.
- Wang, Z.B. & Lodder, Q.L., 2019. Sediment exchange between the Wadden Sea and North Sea Coast, Modelling based on ASMITA, Deltares, Report 1220339-008-ZKS-006.